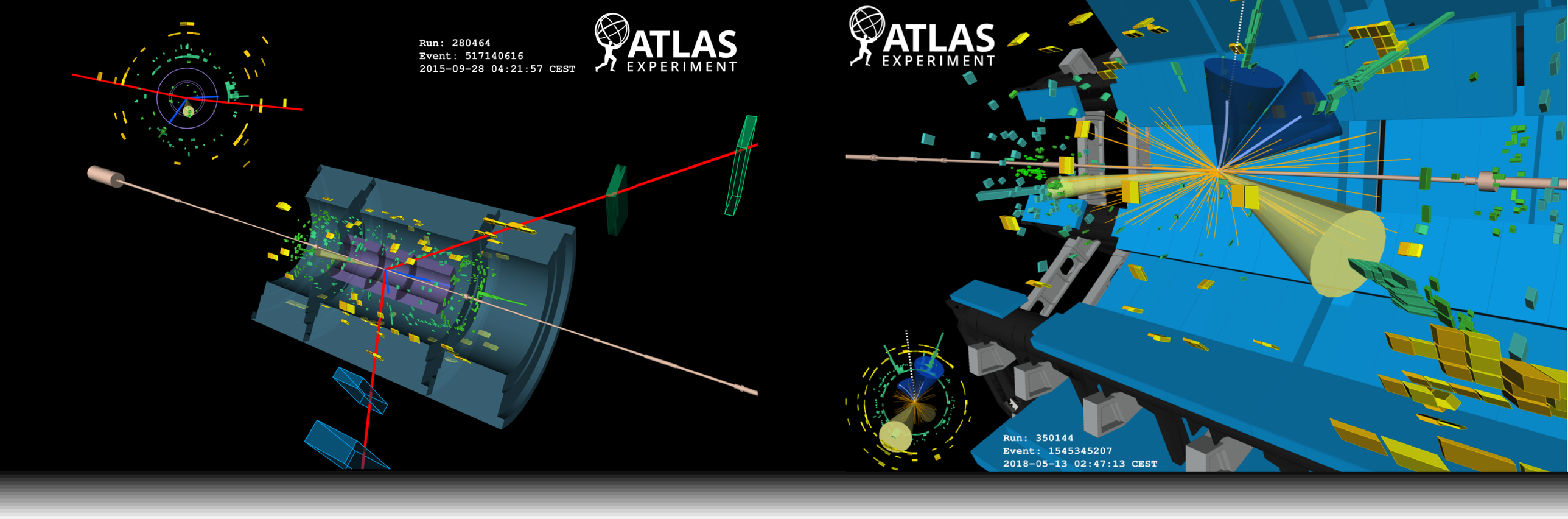

Measurements of Higgs boson properties with the ATLAS detector

Trevor Vickey
on behalf of the ATLAS Collaboration

July 19, 2023

Lepton-Photon 2023 — Melbourne, Australia

ATLAS EXPERIMENT

University of Sheffield

Outline

Higgs Mass

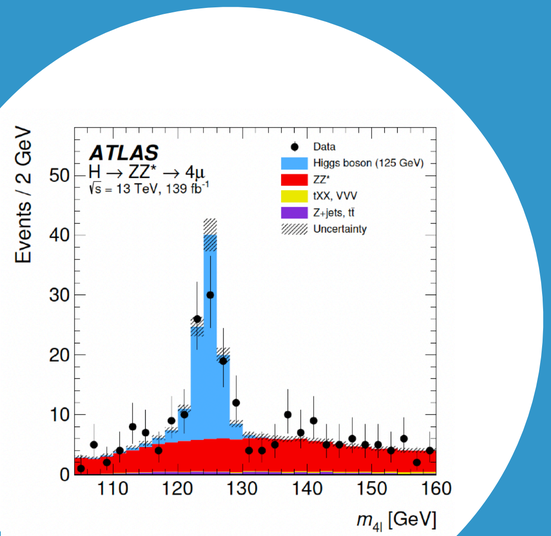

Higgs Width

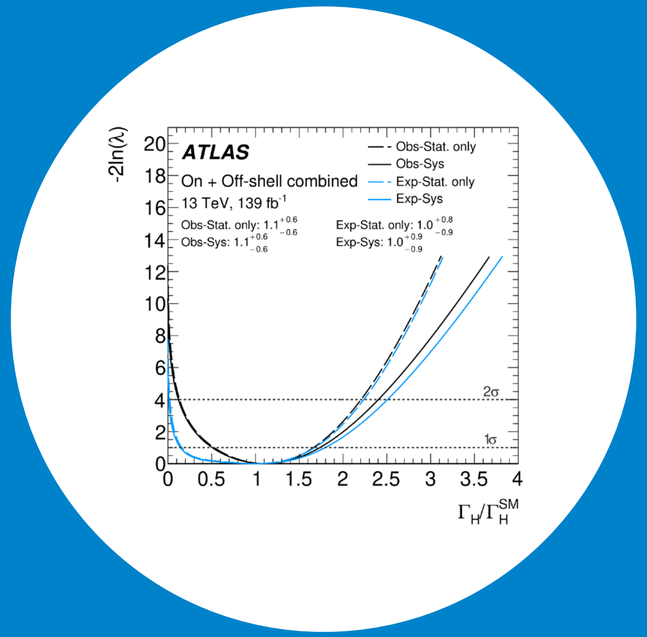

Higgs Spin / CP

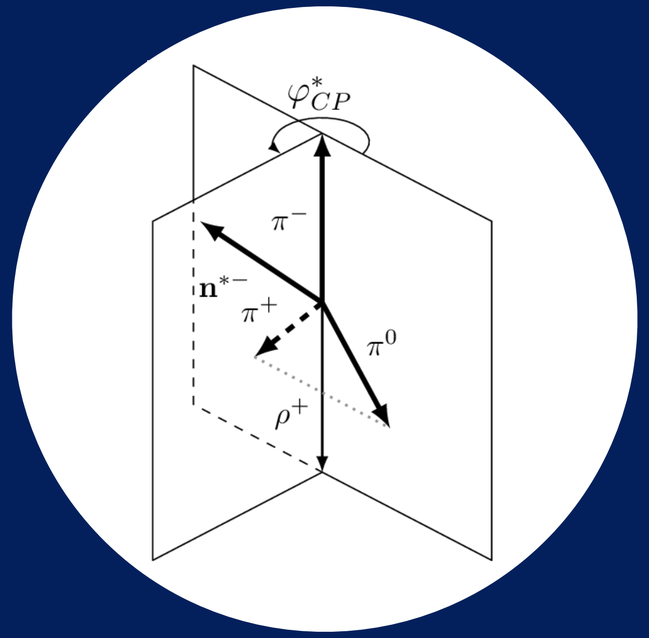

Phys. Lett. B 843 (2023) 137880

Higgs Boson Mass Measurements

- The latest ATLAS H → ZZ* → 4ℓ analysis (ℓ = e or μ):
  - Profits from an increased data sample (full Run-2 dataset of 139 fb^{-1}), includes a new high-precision muon momentum calibration,
  - exploits a neural-network-based classifier for the signal versus background discrimination (improves measurement precision by ~2%) and the inclusion of the event-by-event invariant mass resolution in the analytical model used to fit the data (reducing the total expected uncertainty on m_H by ~1%).

Full Run-2 result: $m_H = 124.99 \pm 0.18\,(\text{stat.}) \pm 0.04\,(\text{syst.}) = 124.99 \pm 0.19\,\text{GeV}$

Run-1 + Run-2 result: $m_H = 124.94 \pm 0.17\,(\text{stat.}) \pm 0.03\,(\text{syst.}) = 124.94 \pm 0.18\,\text{GeV}$

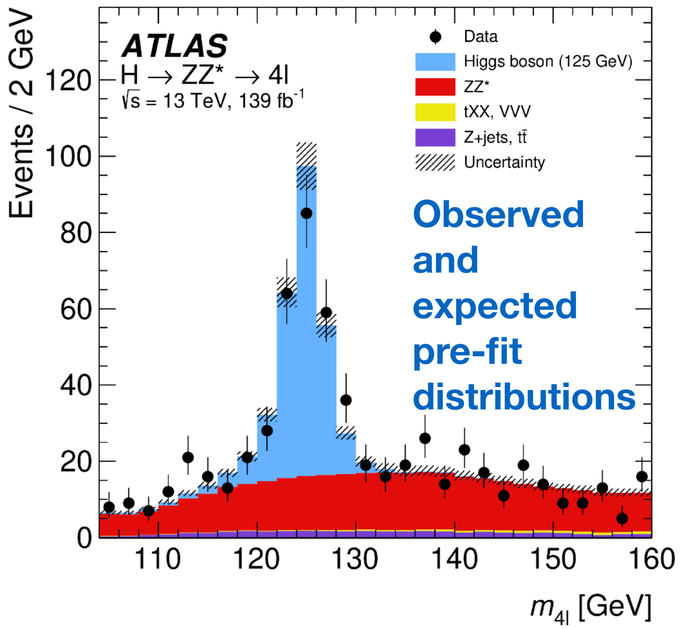

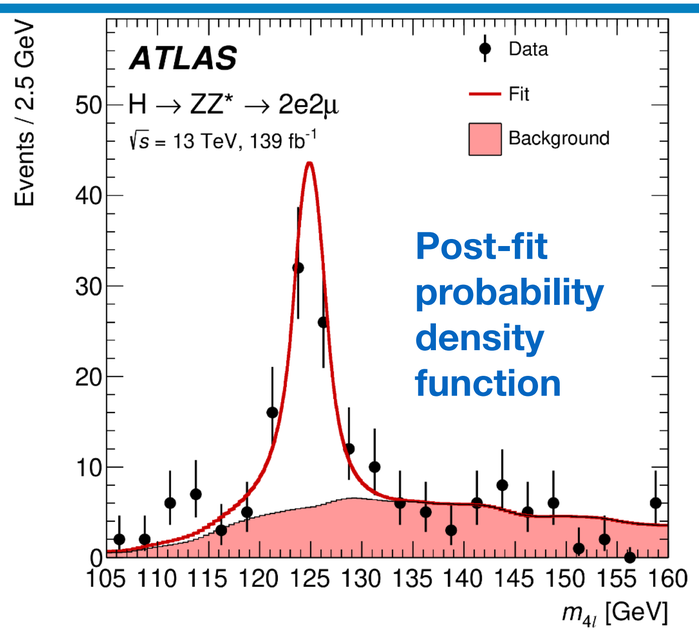

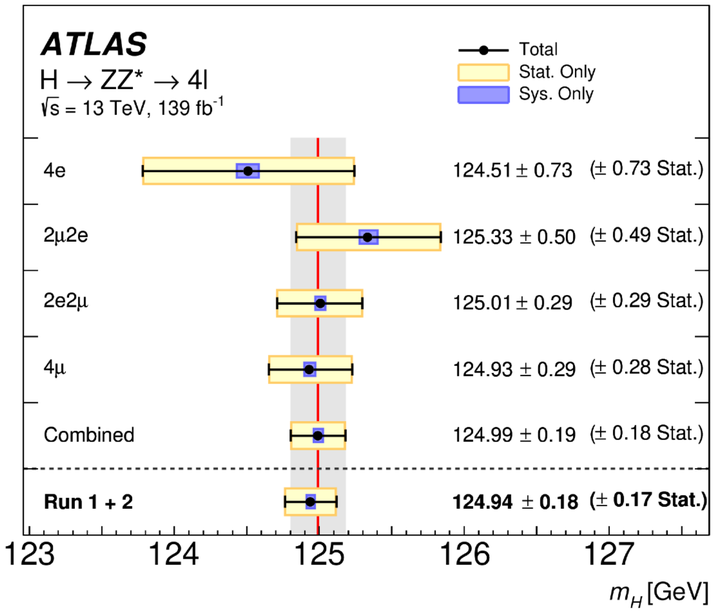

Higgs Boson Mass Measurements

- This latest mass measurement in the Higgs to γγ channels benefits from:
  - An increased data sample (full Run-2 dataset of 140 fb^{-1}), and a new photon reconstruction algorithm with better energy resolution,
  - an improved estimation of the photon energy scale with reduced uncertainties—total systematic uncertainty now down to 90 MeV as compared to an earlier result with 340 MeV (Phys. Lett. B 784 (2018) 345)

Full Run-2 result: $m_H = 125.17 \pm 0.11\,(\text{stat.}) \pm 0.09\,(\text{syst.}) = 125.17 \pm 0.14\,\text{GeV}$

Run-1 + Run-2 result: $m_H = 125.22 \pm 0.11\,(\text{stat.}) \pm 0.09\,(\text{syst.}) = 125.22 \pm 0.14\,\text{GeV}$

Most precise Higgs mass measurement from a single channel!

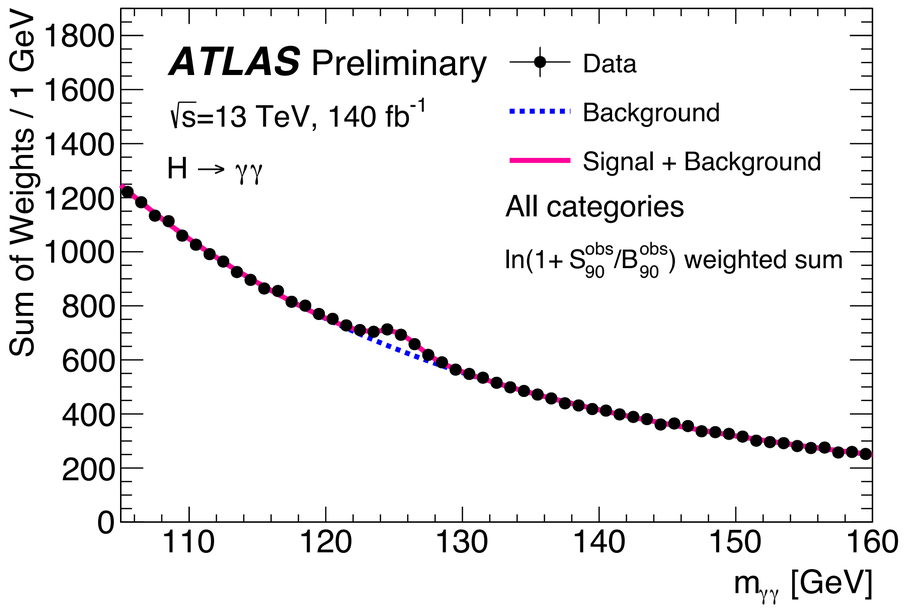

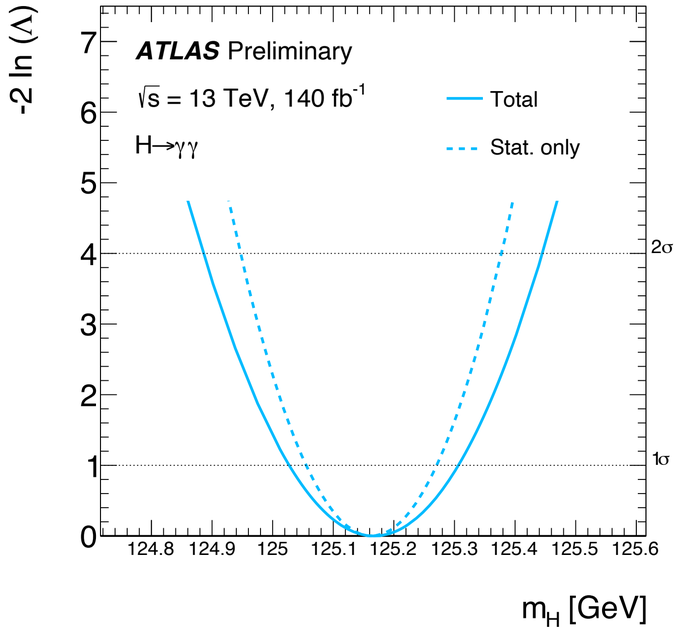

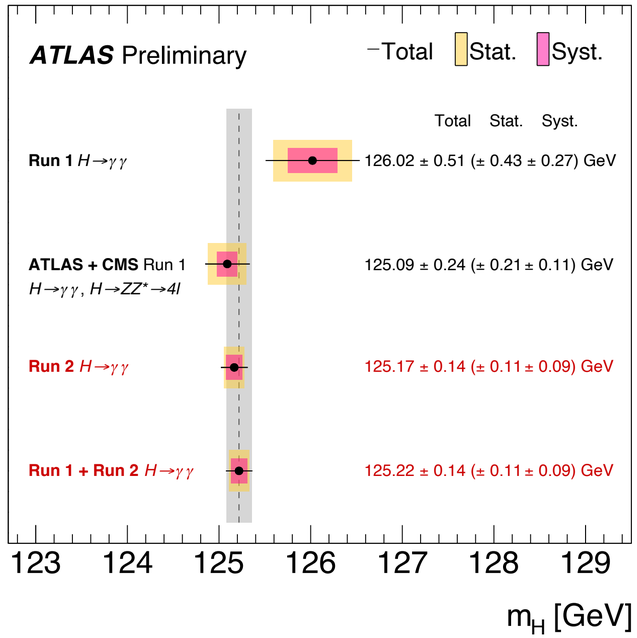

Higgs Boson Mass Combination

- Measurement combines the latest results in the H → ZZ* → 4ℓ and H → γγ decay channels
- Result based on 140 fb^{-1} of pp collision data collected at a center of mass energy of 13 TeV during Run-2

Full Run-2 result: $m_H = 125.10 \pm 0.09\,(\text{stat.}) \pm 0.07\,(\text{syst.}) = 125.10 \pm 0.11\,\text{GeV}$

Run-1 + Run-2 result: $m_H = 125.11 \pm 0.09\,(\text{stat.}) \pm 0.06\,(\text{syst.}) = 125.11 \pm 0.11\,\text{GeV}$

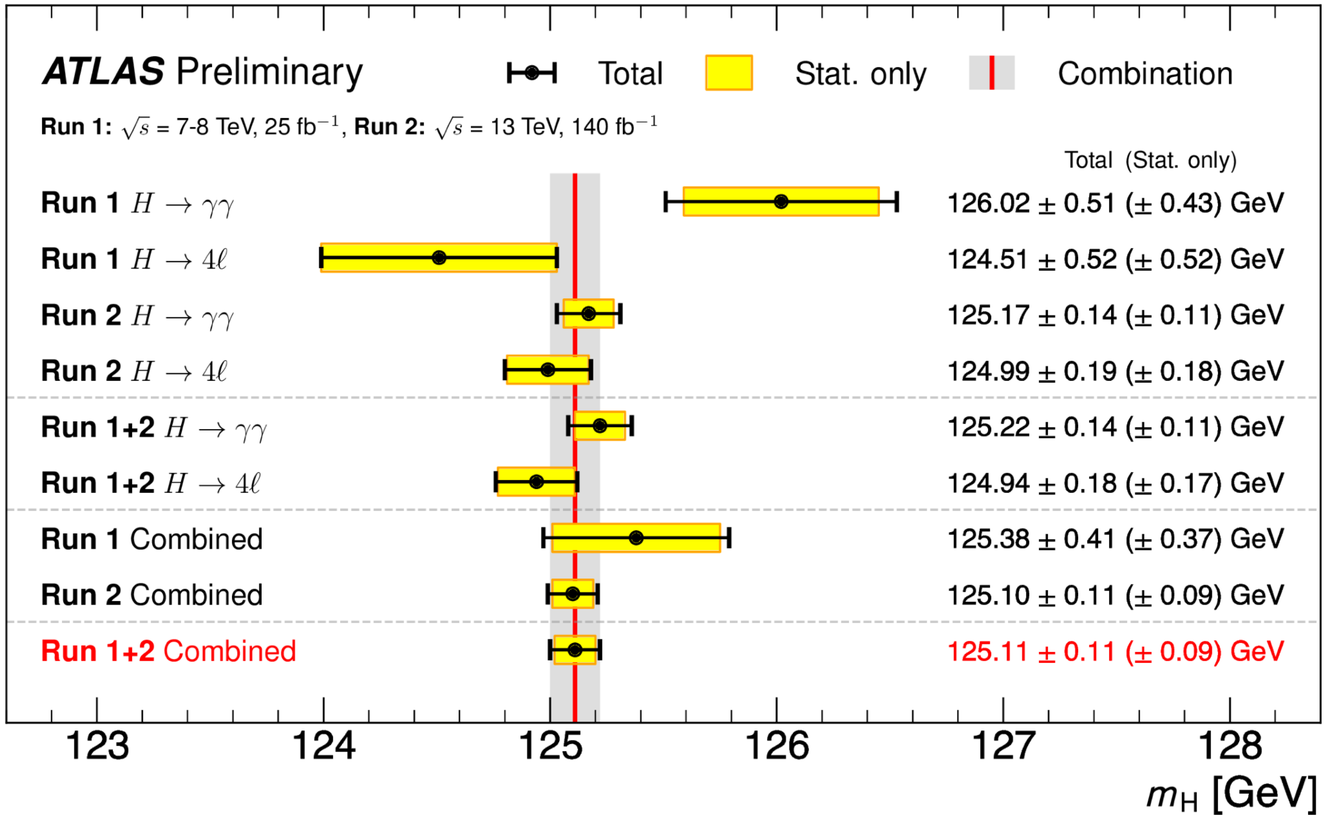

Currently the most precise measurement of the Higgs boson mass, with an uncertainty of 110 MeV!

arXiv:2304.01532

Determination of the Higgs Boson Width

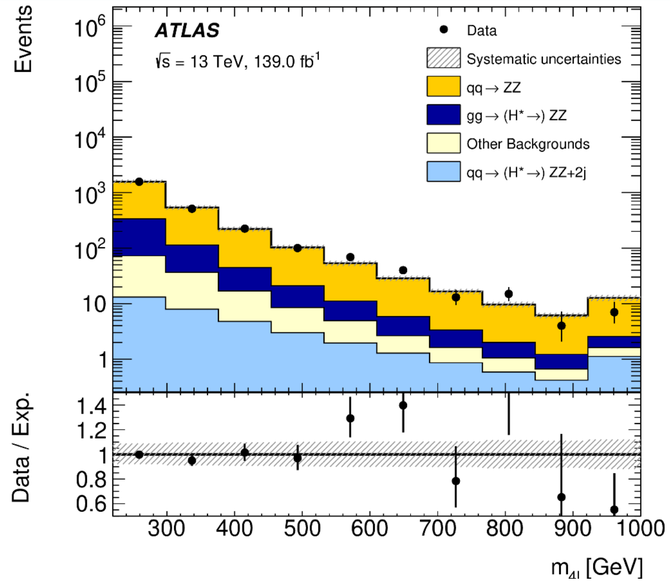

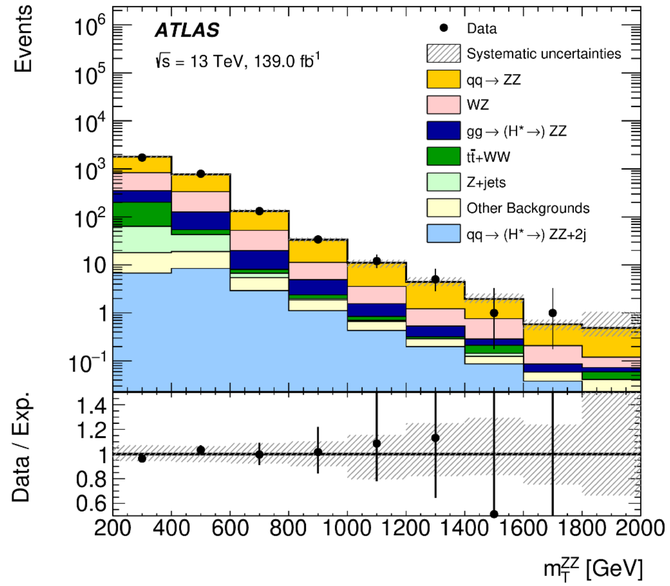

- Predicted Higgs width of 4.1 MeV is much smaller than the detector resolution
- This 4ℓ and $2\ell\,2\nu$ ZZ combination exploits the independence of off-shell cross section on Γ_H and relies on identical on-shell and off-shell Higgs couplings to determine Γ_H from measurements of $\mu_{\text{off-shell}}$ and $\mu_{\text{on-shell}}$

$$\sigma^{\text{on-shell}}_{gg\to H\to VV} \sim \frac{g^2_{ggH} g^2_{HZZ}}{m_H \Gamma_H} \qquad \sigma^{\text{off-shell}}_{gg\to H\to VV} \sim \frac{g^2_{ggH} g^2_{HZZ}}{m^2_{ZZ}}$$

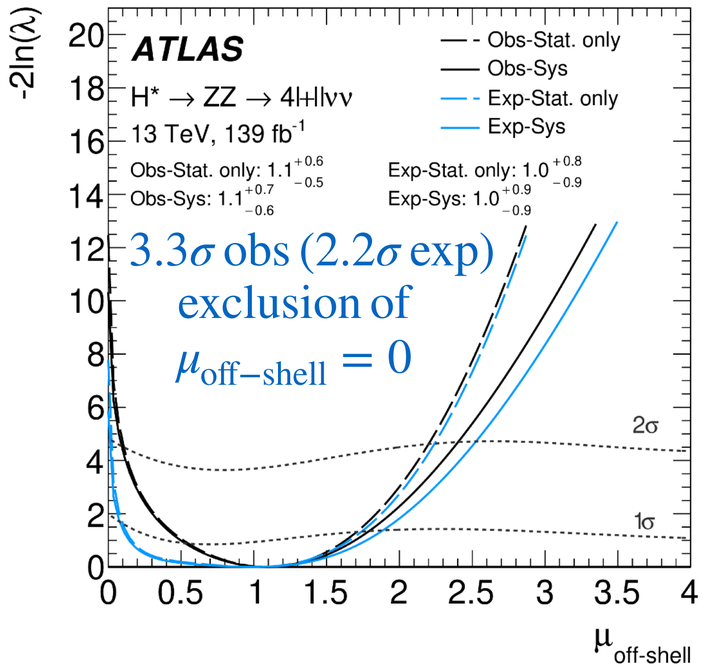

Evidence for off-shell Higgs boson production!

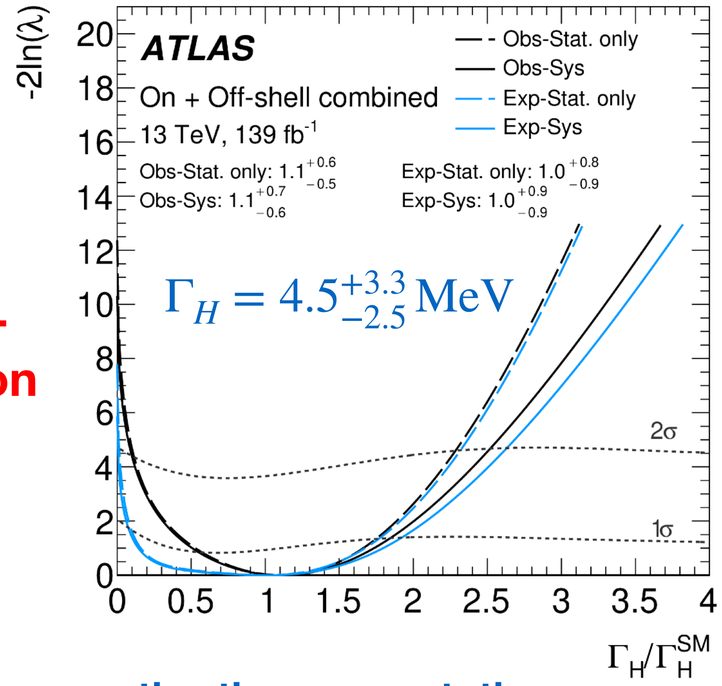

NB: Neyman likelihood profiles shown; ~5-10% more conservative than asymptotic

Eur. Phys. J. C 83 (2023) 563

Measuring CP properties of Higgs boson interactions with τ leptons

- Analysis tests the CP properties of the tau Yukawa coupling, where contributions can be present at tree level
- The CP-mixing angle ϕ_τ is reflected in tau decay kinematics

First ATLAS analysis to use tau decay classification!

- Rejection of the CP-odd hypothesis at 3.4σ (2.1σ expected)

$$\mathcal{L}_{H\tau\tau} = -\frac{m_\tau}{v}\kappa_\tau(\cos\phi_\tau\bar{\tau}\tau + \sin\phi_\tau\bar{\tau}i\gamma_5\tau)H$$

CP-even **CP-odd**

SM case: $\phi_\tau = 0$

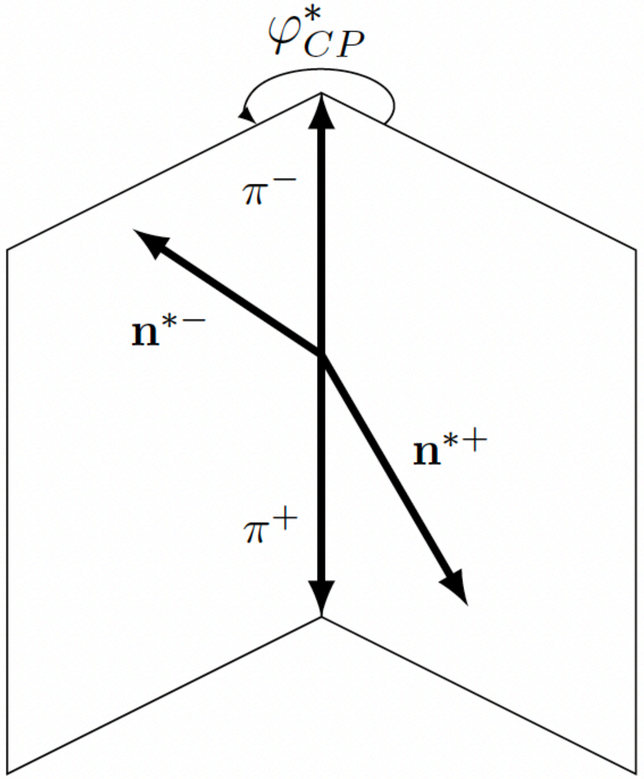

$H \to \tau^+\tau^- \to \pi^+\pi^- + 2\nu$

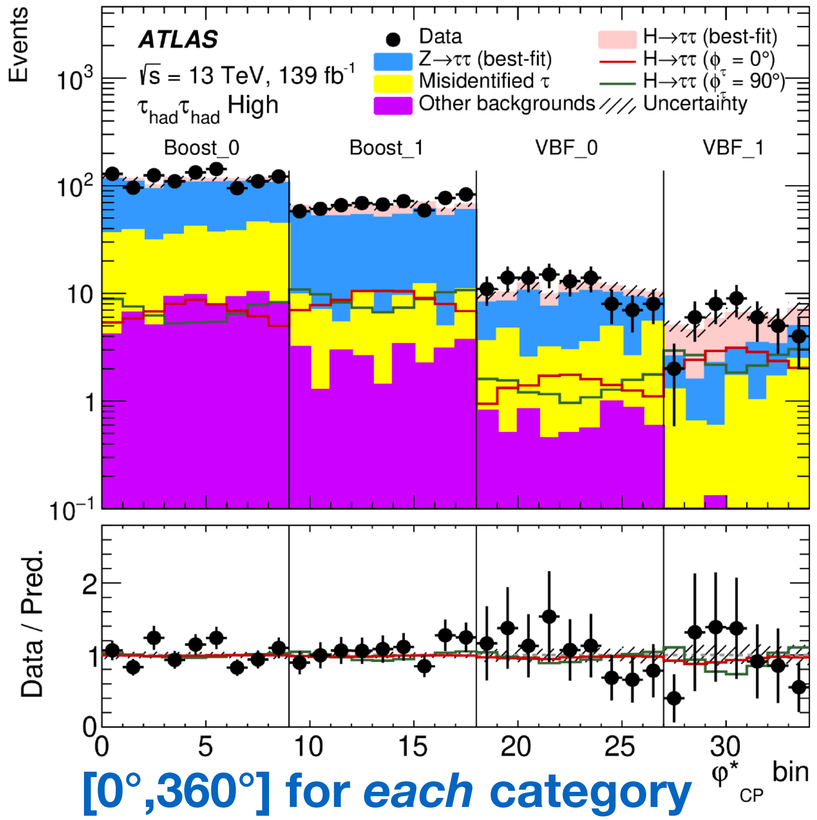

[0°,360°] for *each* category

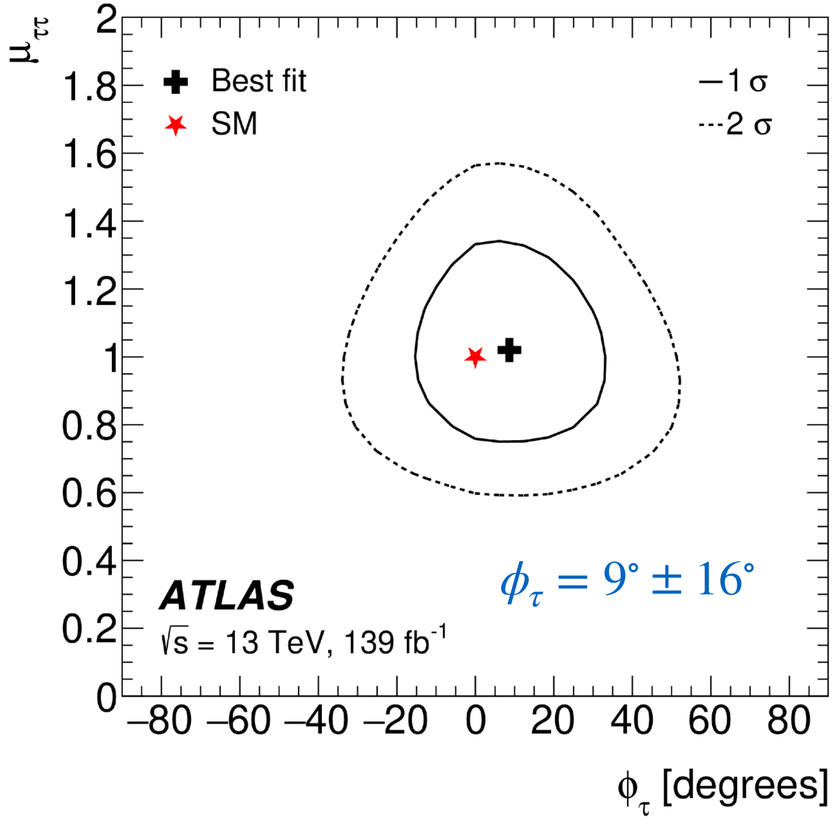

arXiv:2304.09612

Probing the CP-odd Component with H→ZZ*→4ℓ

- Measurement using 139 fb^{-1} of Run-2 data in the 4ℓ final state
- Based on the Effective Field Theory (EFT) approach, using the Optimal Observable (OO) to probe any possible CP-odd component — represents the interference term of the SM+BSM Matrix Elements
- Define two *types* of OOs: some for production (VBF enriched) and others for decay (inclusive)
  - An Optimal Observable for each SMEFT CP-odd Wilson coefficient that is considered

$$OO = \frac{2\Re\left(\mathcal{M}^{*}_{\mathrm{SM}}\mathcal{M}_{\mathrm{BSM}}\right)}{|\mathcal{M}_{\mathrm{SM}}|^{2}}$$

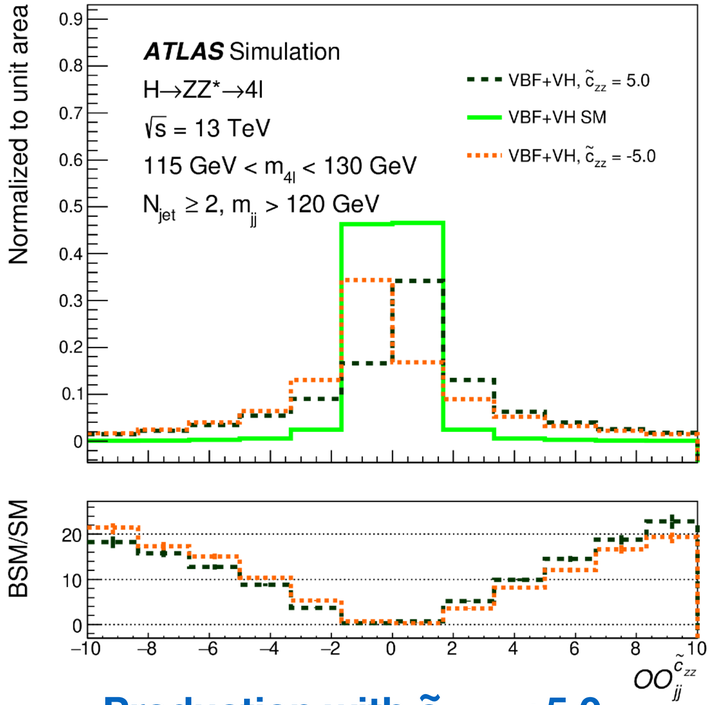

Production with $\tilde{c}_{ZZ}$ = ±5.0

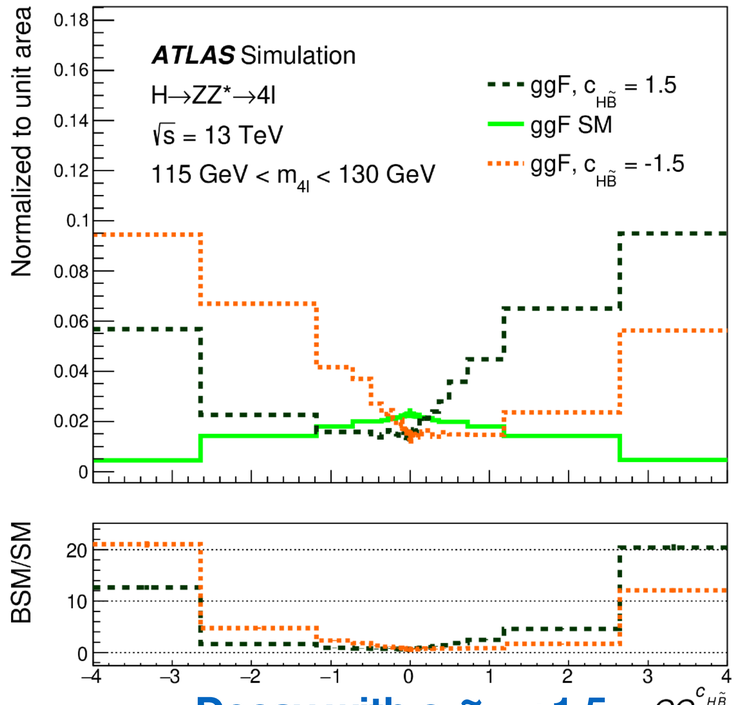

Decay with $c_{H\tilde{B}}$ = ±1.5

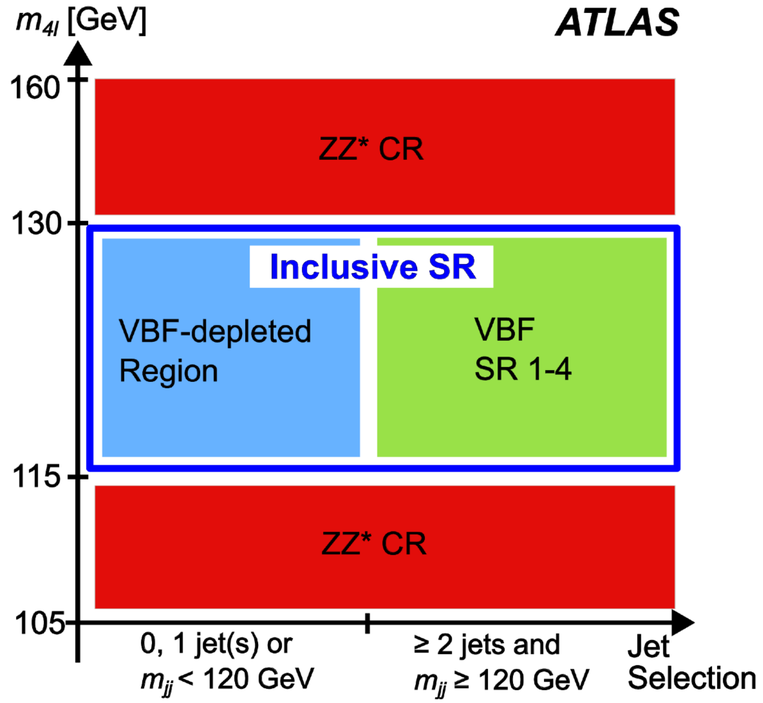

arXiv:2304.09612

Probing the CP-odd Component with H→ZZ*→4ℓ

- A neural-network training is performed to enhance the VBF purity (a total of four VBF signal regions are defined)
- Different types of fits are performed:
  - One each for production, decay, and combined
  - Unfolded distributions of the OO are also provided, for reinterpretations

Results are consistent with CP-even of the Standard Model

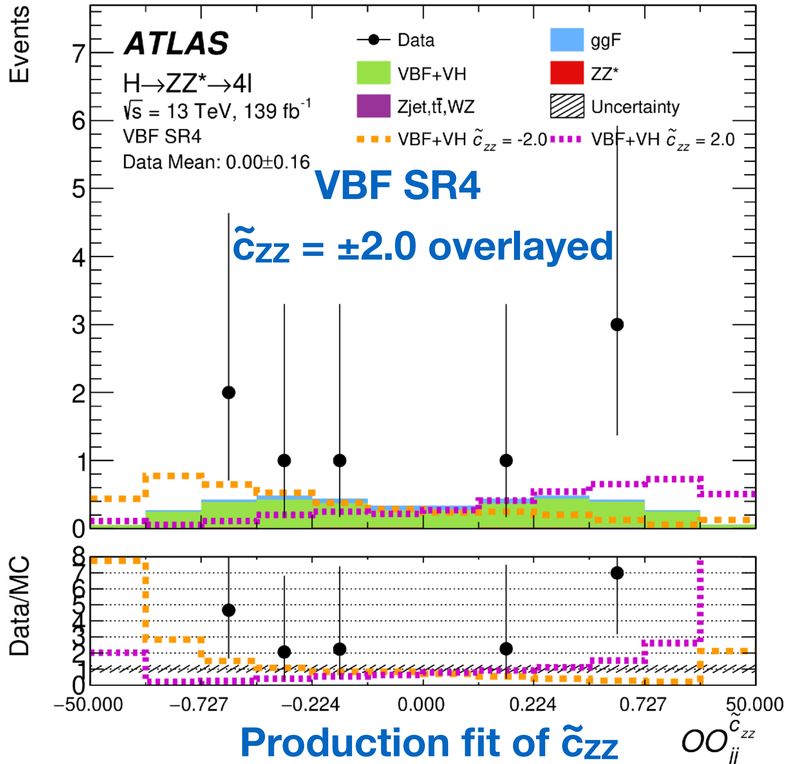

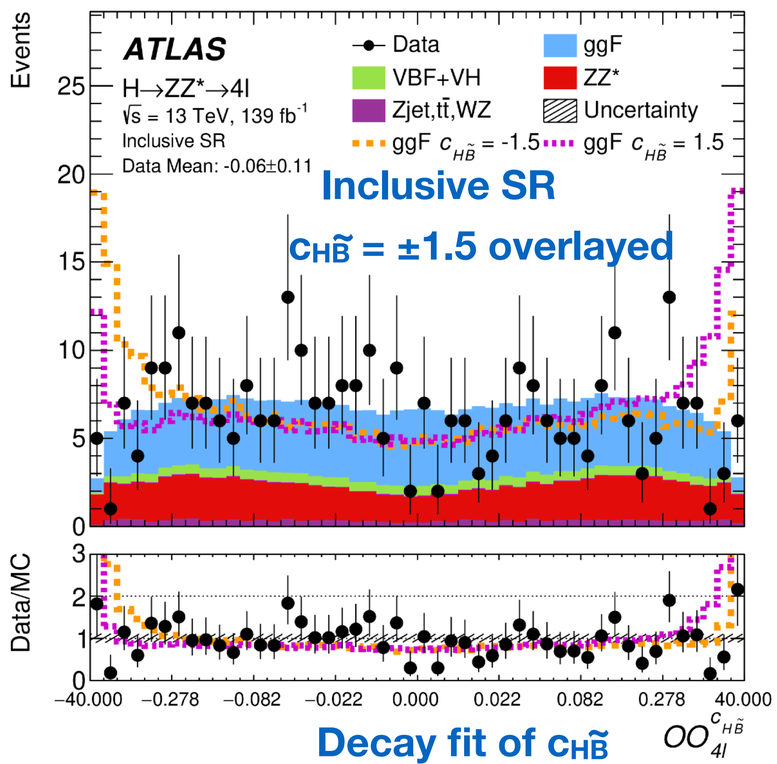

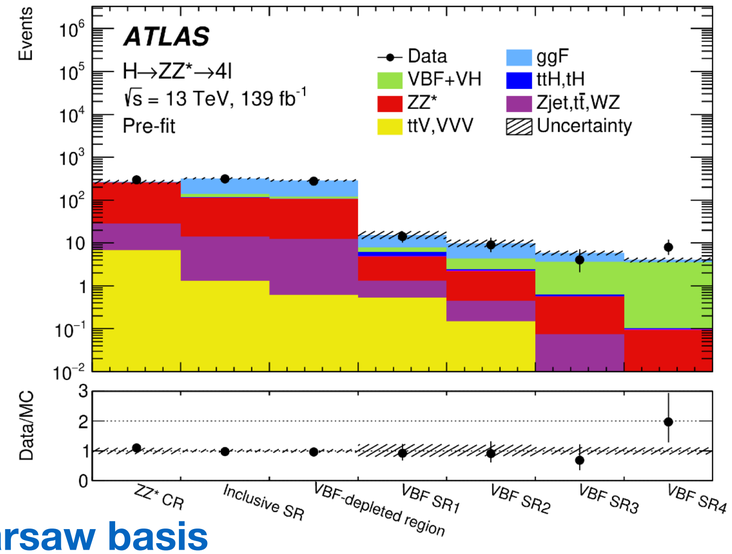

Warsaw basis

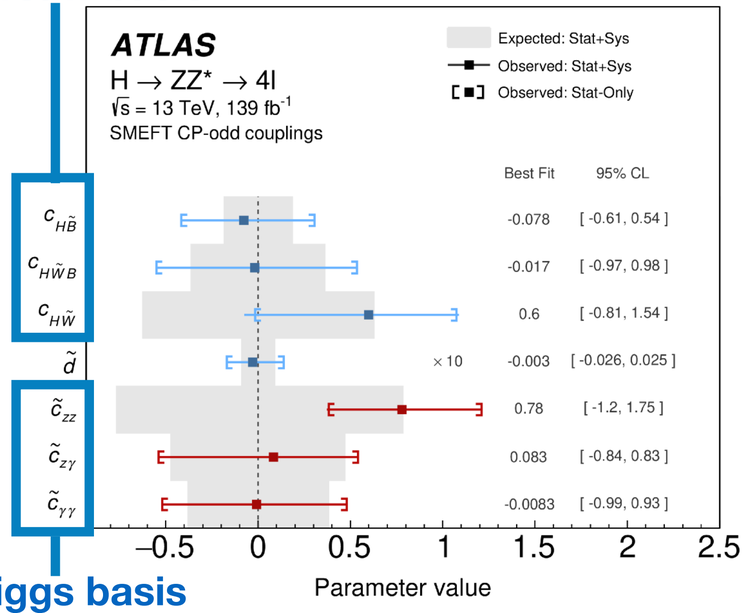

arXiv:2303.05974

Probing the CP Nature of the Higgs-top Yukawa Coupling

- Measure the CP structure of H-top interaction in ttH and tH production using H→bb decays
- Uses lepton+jets (includes a boosted region) and di-lepton channels
  - BDT is trained for event categorization
  - Two dedicated CP-sensitive variables are defined using top-quark kinematic information (the observables)
  - Boosted region uses BDT for CP-even/odd separation

$$\mathcal{L}_{t\bar{t}H} = -\kappa_t' y_t \phi \bar{\psi}_t (\cos\alpha + i\gamma_5 \sin\alpha)\psi_t$$

CP-even **CP-odd**

SM case: κ'$_t$ = 1 and α = 0

$$b_2 = \frac{(\vec{p}_1 \times \hat{z}) \cdot (\vec{p}_2 \times \hat{z})}{|\vec{p}_1||\vec{p}_2|}$$

$$b_4 = \frac{(\vec{p}_1 \cdot \hat{z})(\vec{p}_2 \cdot \hat{z})}{|\vec{p}_1||\vec{p}_2|}$$

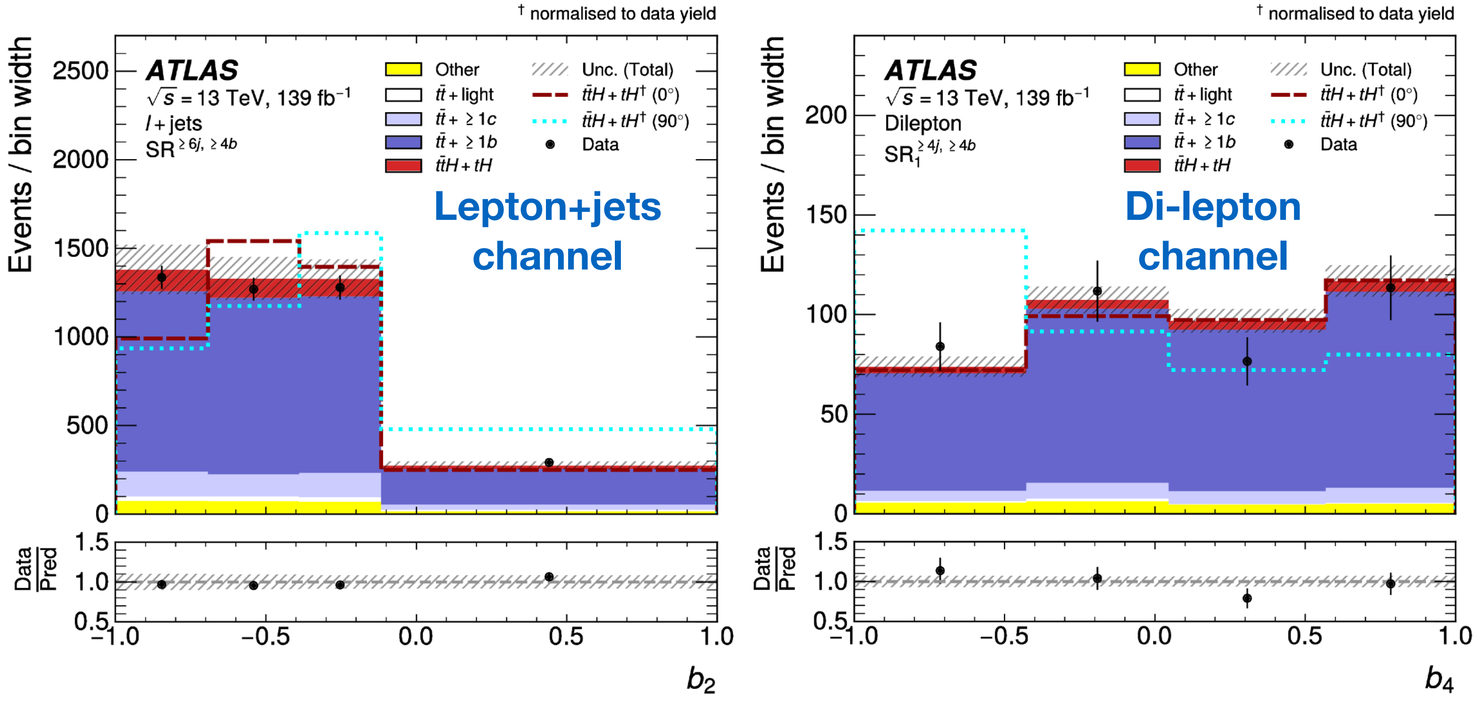

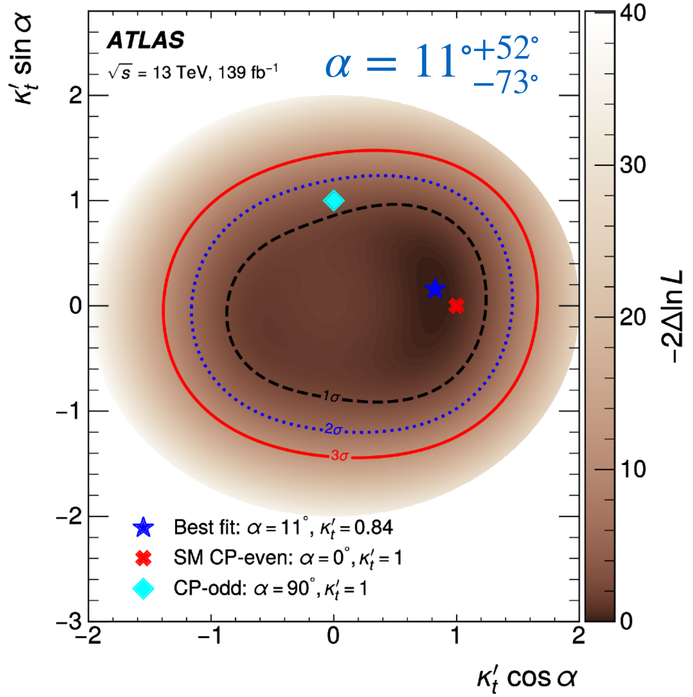

Summary

- ATLAS measurements of Higgs boson properties have been presented: mass, width, CP

- The most precise Higgs boson mass measurement in a single channel has been obtained by combining the Run-1 (7 and 8 TeV) and Run-2 (13 TeV) results from $H \to \gamma\gamma$ decays:

$$m_H = 125.22 \pm 0.11\,(\text{stat.}) \pm 0.09\,(\text{syst.}) = 125.22 \pm 0.14\,\text{GeV}$$

- Results from the full Run-2 dataset, using the $H \to ZZ^* \to 4\ell$ and $H \to \gamma\gamma$ decay channels, are combined with the Higgs boson mass measurements performed on Run-1 data. The combined result is:

$$m_H = 125.11 \pm 0.09\,(\text{stat.}) \pm 0.06\,(\text{syst.}) = 125.11 \pm 0.11\,\text{GeV}$$

  - This currently represents the most precise measurement of the Higgs boson mass, reaching a 0.87 per mille accuracy on this fundamental quantity.

- The Higgs boson width is measured to be: $\Gamma_H = 4.5^{+3.3}_{-2.5}\,\text{MeV}$

- CP properties of the Higgs boson have been studied in various channels and found to be consistent with the Standard Model
  - A pure CP-odd contribution is excluded for H-tau and H-top interactions
  - There is still room for a CP mixture

- Analysis of Run-3 data is on-going, and we're excited to learn even more about the Higgs boson and its properties

Back-up

Higgs Spin

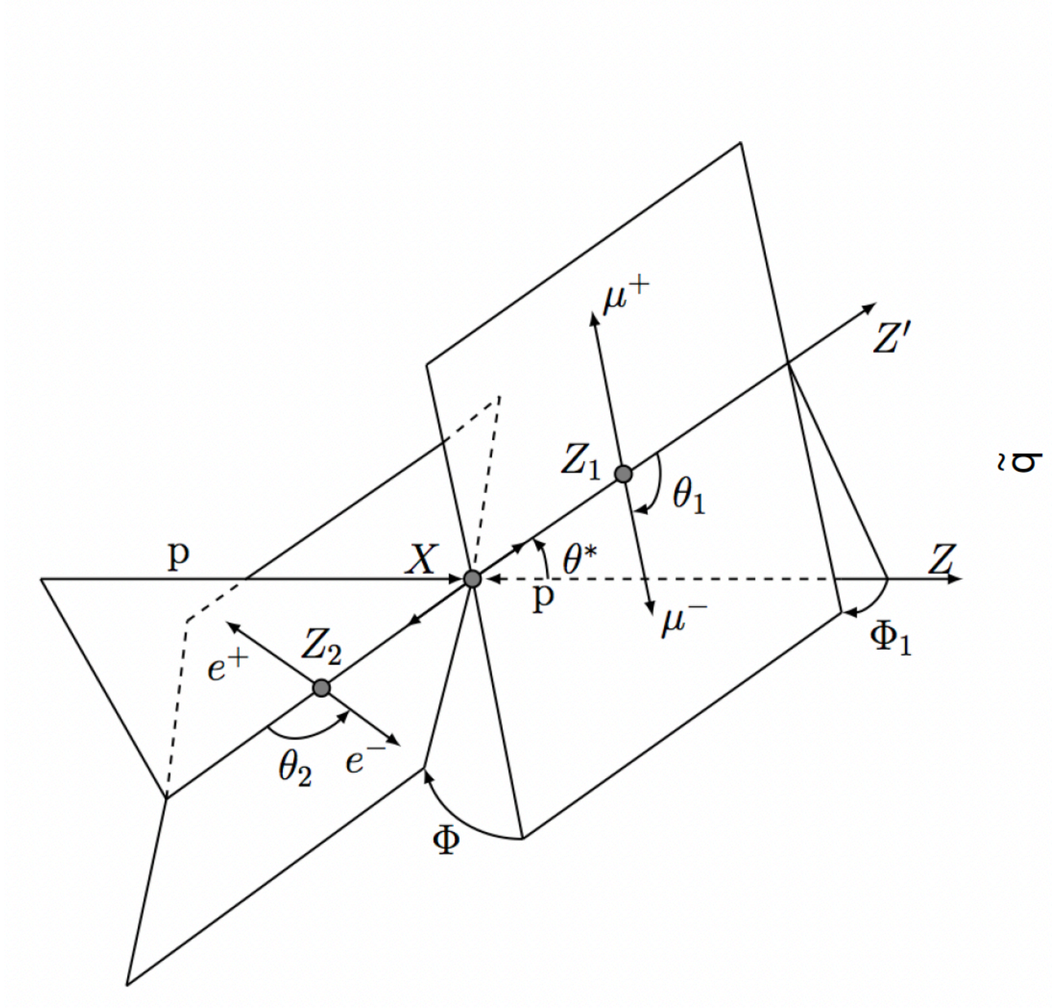

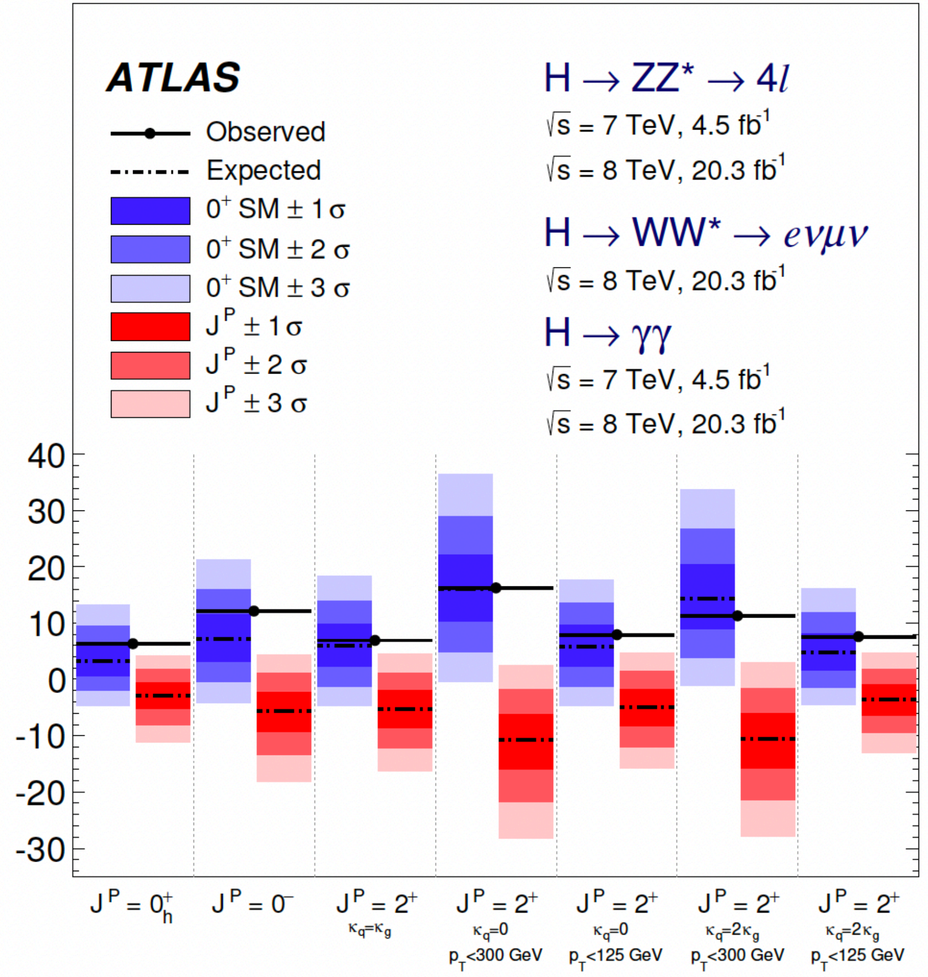

Eur. Phys. J. C75 (2015) 476

Higgs mass in the 4ℓ channel

- Pre-fit yields (between 115 and 130 GeV) and largest contributions to systematics on m_H:

Final state	Higgs	ZZ, tXX, VVV	Reducible backgrounds	Expected total yield	Observed yield	S/B
4μ	78 ± 5	38.7 ± 2.2	2.84 ± 0.17	120 ± 5	115	1.89
$2e2\mu$	53.4 ± 3.2	26.7 ± 1.4	3.02 ± 0.19	83.1 ± 3.5	94	1.80
$2\mu2e$	41.2 ± 3.0	17.9 ± 1.3	3.4 ± 0.5	62.5 ± 3.3	59	1.93
$4e$	36.2 ± 2.7	15.7 ± 1.6	2.83 ± 0.35	54.8 ± 3.2	45	1.95
Total	209 ± 13	99 ± 6	12.2 ± 0.9	321 ± 14	313	1.88

Systematic Uncertainty	Contribution [MeV]
Muon momentum scale	± 28
Electron energy scale	± 19
Signal-process theory	± 14

Compared to previous Run-2 result:

Statistical uncertainty reduced by a factor of 2,

Systematic uncertainty reduced by ~20%

Higgs mass in the 4ℓ channel

- Signal-background discrimination done using a deep feed-forward neural network (D_{NN})
- The event-level m_H resolution, σ_i, is estimated using a quantile regression neural network (QRNN) trained on signal MC events using the p_T, η, and ϕ of the individual leptons, as well as the constrained four-lepton momentum and its uncertainty as inputs.

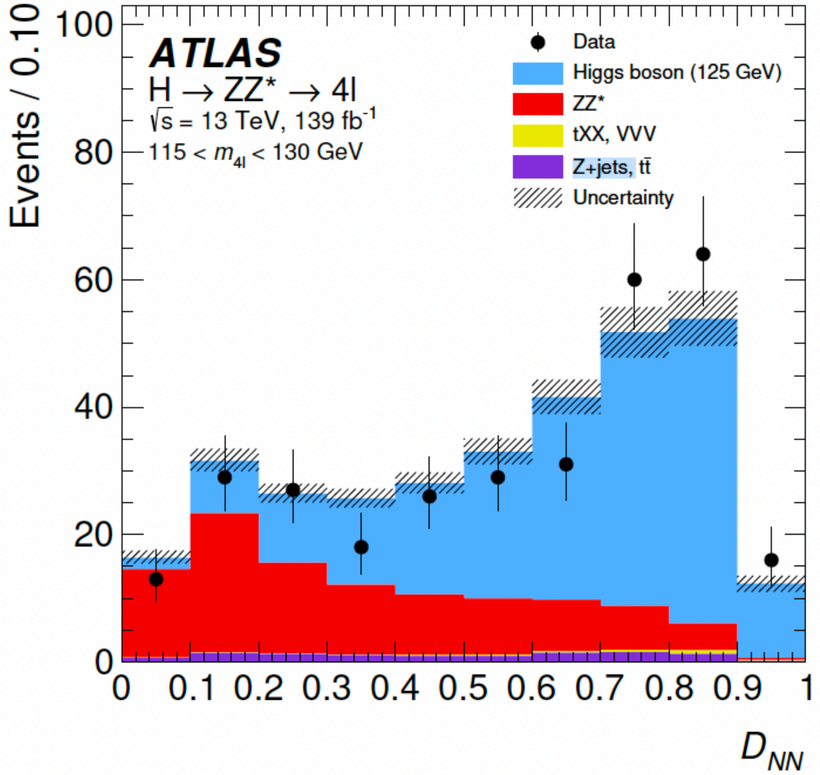

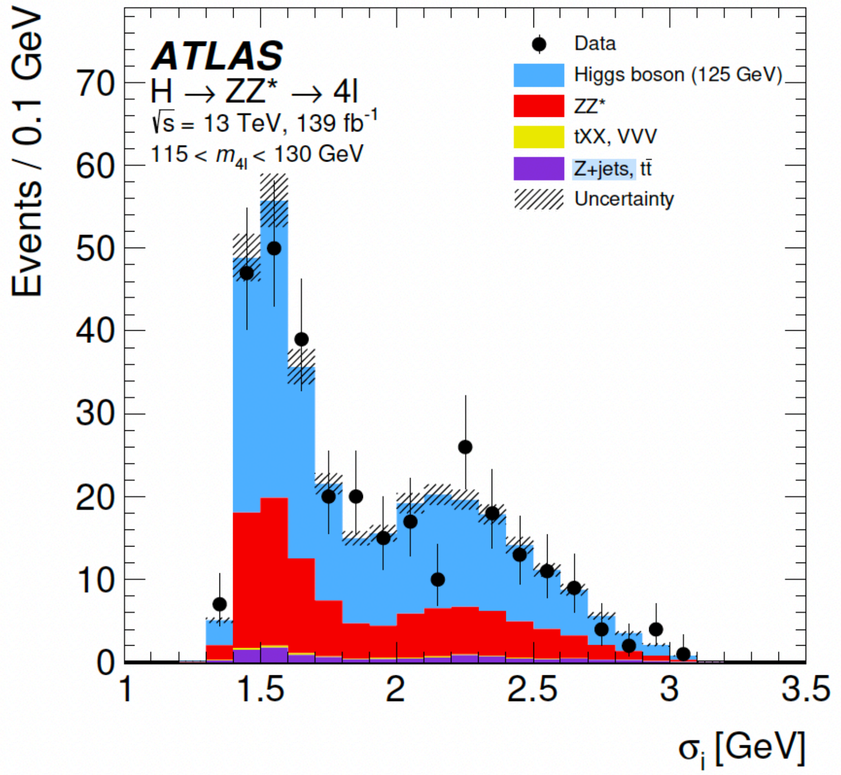

Higgs mass in the γγ channel

- Background is the γγ continuum (non-resonant $pp \rightarrow \gamma\gamma$ + n parton (n ≥ 0))
- Sources of systematic uncertainties for the Higgs mass measurement in the γγ channel

Source	Systematic uncertainty in m_H [MeV]
Photon energy scale	±83
$Z \rightarrow e^+e^-$ calibration	±59
E_T-dependent electron energy scale	±44
$e^{\pm} \rightarrow \gamma$ extrapolation	±30
Conversion modelling	±24
Signal-background interference	±26
Resolution	±15
Background model	±14
Selection of the diphoton production vertex	±5
Signal model	±1
Total	±90

Higgs mass in the $\gamma\gamma$ channel

- Benefits from a new auxiliary measurement (**linearity fit**) of the dependence of the data-to-MC electron energy scale corrections as a function of the electron E_T
- Previous mass measurement, only eta-dependent energy scale factors were derived
  - Done by comparing the position of the peak of the invariant mass distribution of e^+e^- pairs from Z boson decays to that predicted by the simulation.
  - Possible E_T-dependence of the data-to-MC energy scale correction was accounted for as a systematic uncertainty (arising from the various sources belonging to the E_T-dependent electron energy scale)
- New approach exploits the larger sample of $Z \rightarrow e^+e^-$ decays collected in 2015–2018 to derive residual data-to-MC energy scale factors in bins of electron E_T within broad eta regions.
  - The measurement of these additional scale factors is used to constrain the E_T-dependent electron energy scale systematic uncertainties
- The additional constraints and correlation of the systematic uncertainties from the **linearity fit** are propagated to the Higgs boson mass measurement by implementing in the likelihood function a unique multivariate Gaussian constraint term defined from the covariance matrix returned by the **linearity fit**

Higgs mass in the γγ channel

Impact of linearity fit:

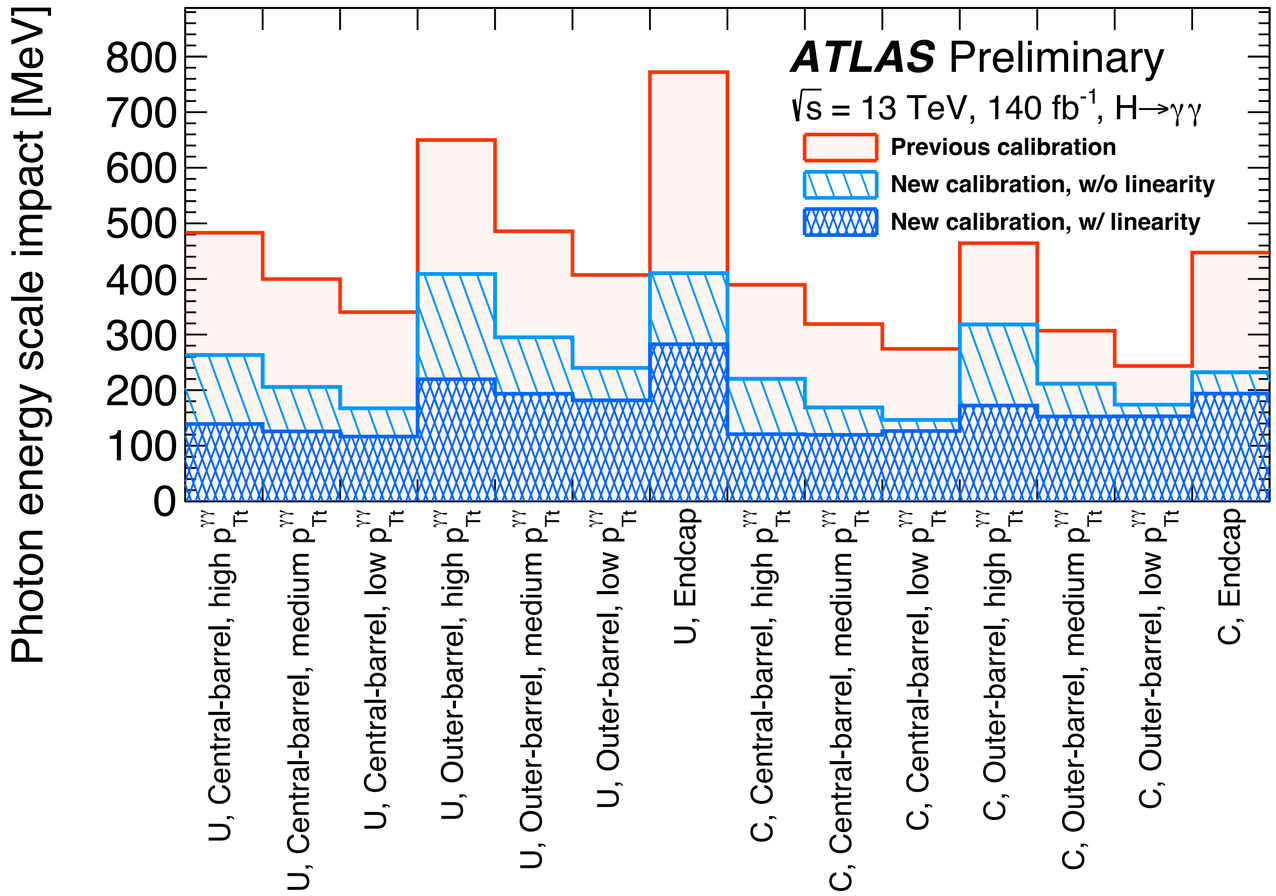

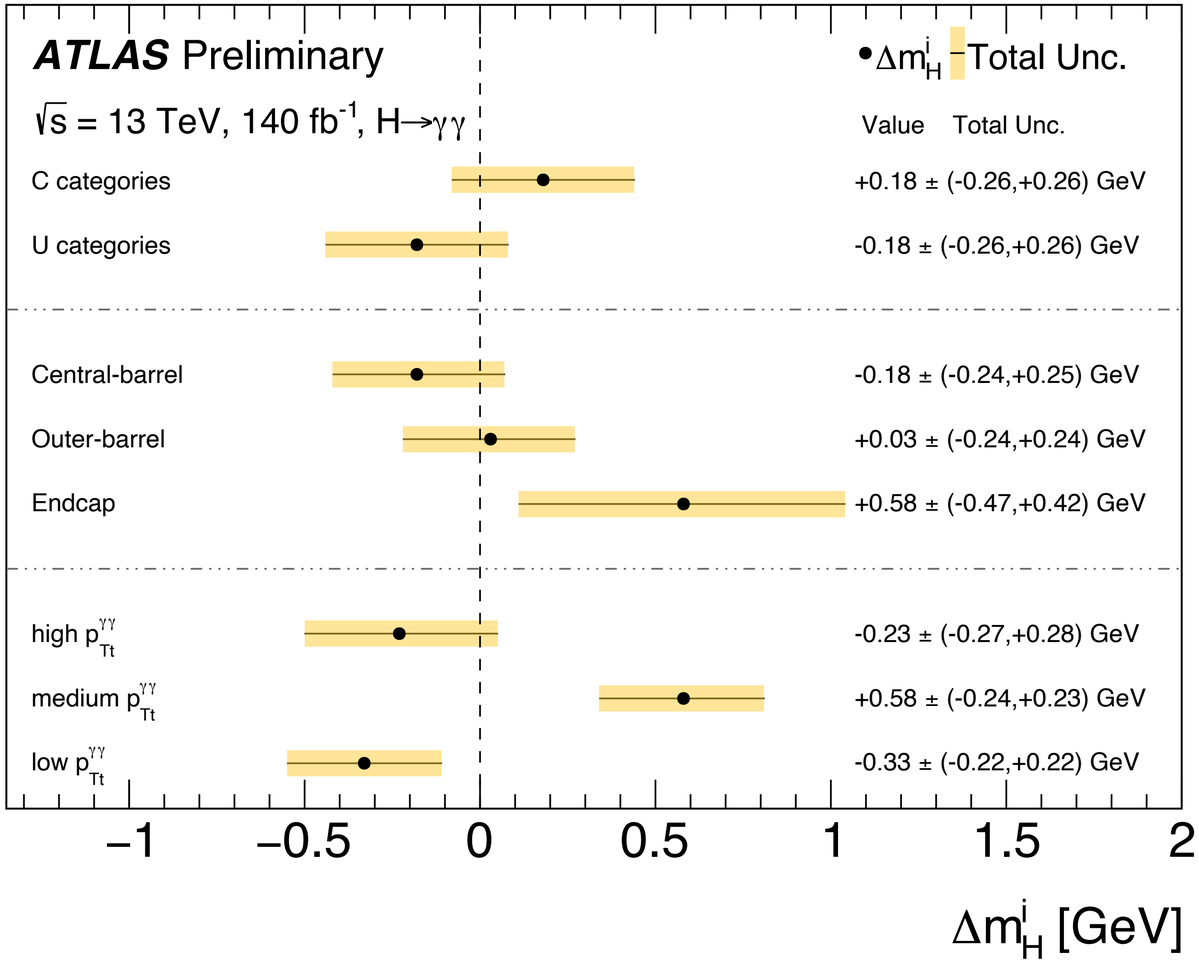

U-type events: No photon candidates after e^+e^- conversion

C-type events: Events with one or two γ → e^+e^- candidates

Higgs Mass Combination — −2 lnΛ

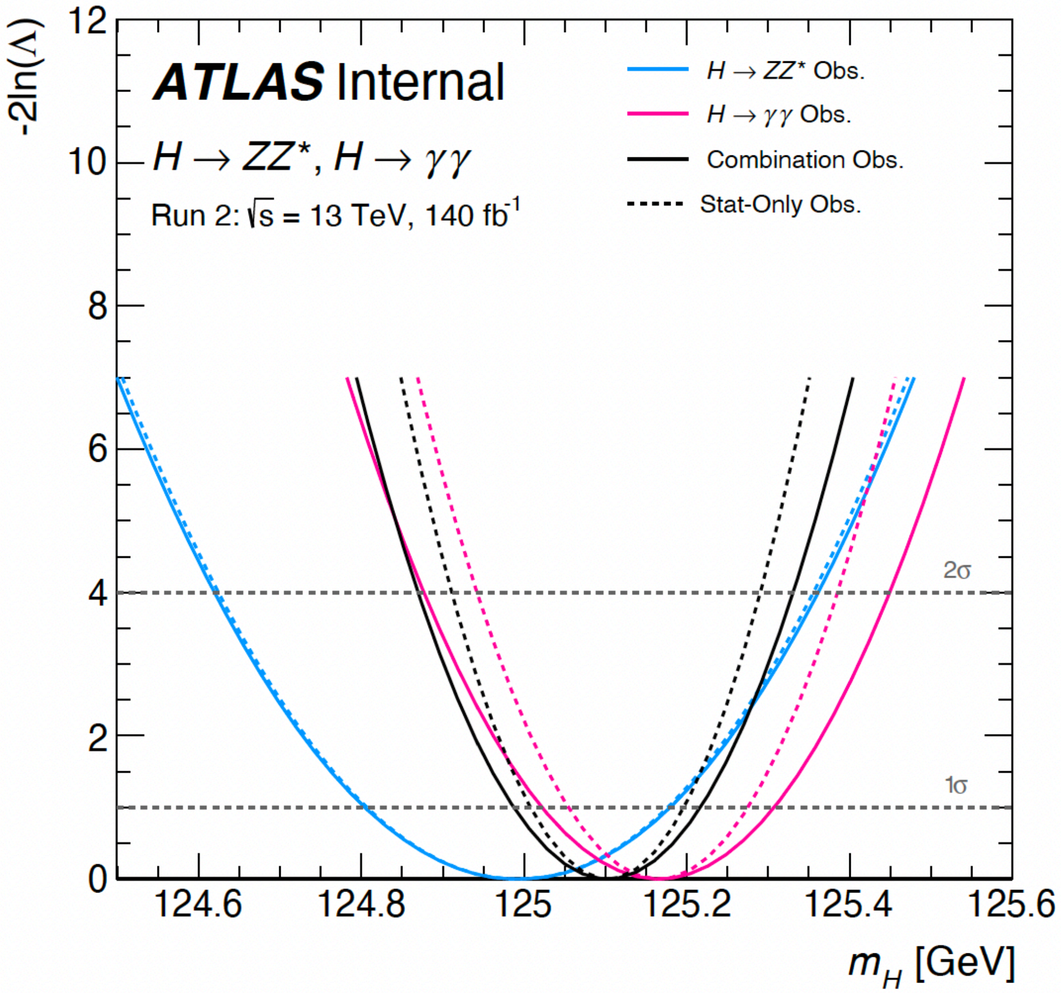

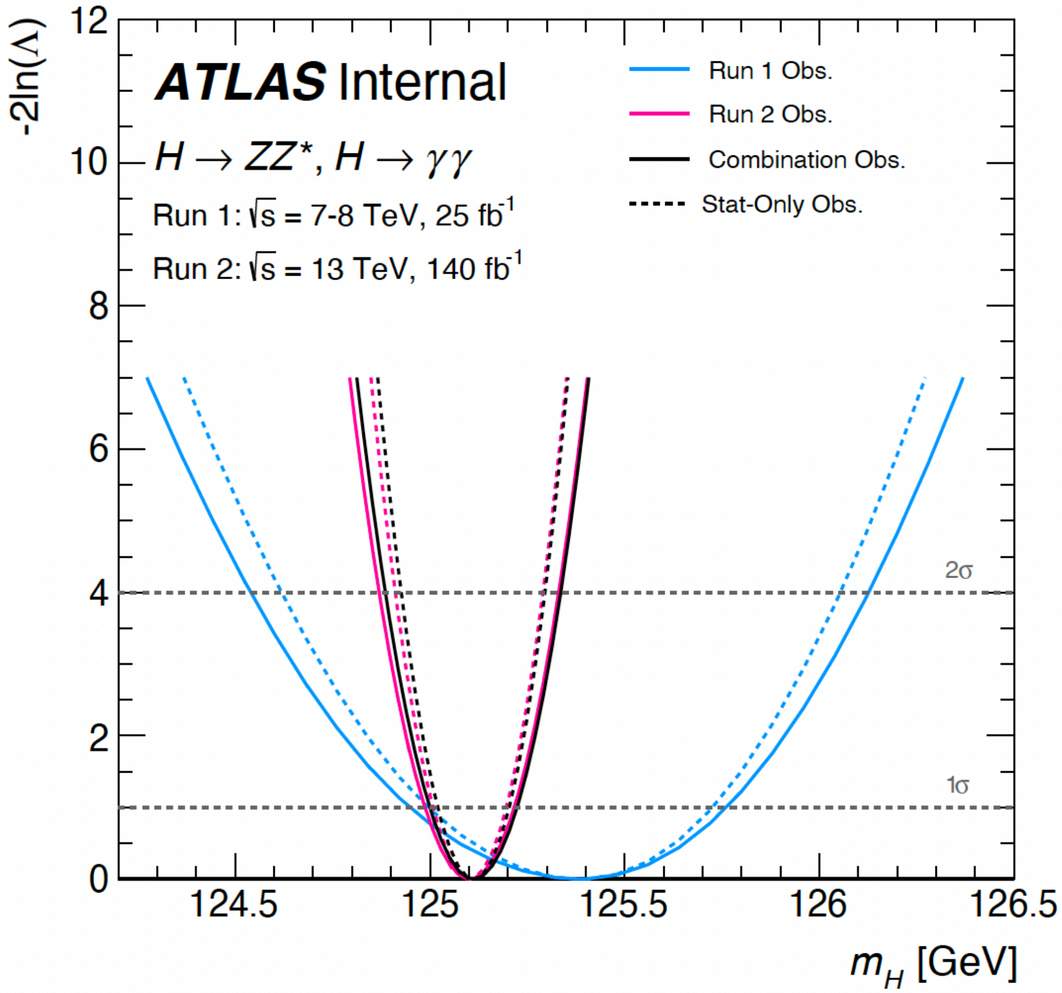

Higgs Mass Combination — Systematics

- Most of the systematics have been kept uncorrelated between the 4 measurements, with the exception of the Z→ee scale (more details in the CONF Note: ATLAS-CONF-2023-037)

Source	Systematic uncertainty on m_H [MeV]
$Z \to ee$ calibration	43
p_{T}-dependent e energy scale	28
Lateral shower shape	18
$H \to \gamma\gamma$ interference bias	16
$H \to \gamma\gamma$ conversion reconstruction	14
$H \to \gamma\gamma$ background modelling	10
Muon momentum scale	7
e/γ energy resolution	7
All other systematic uncertainties	8

Table 1: Impact of the main sources of systematic uncertainty on the Higgs boson mass m_H measurement from the combination of the $H \to ZZ^* \to 4\ell$ and $H \to \gamma\gamma$ final states using Run 2 data. The systematic uncertainties associated with the combination of Run 1 and Run 2 data are comparable.

Off-Shell Higgs Production

- Observed and expected yields in the 4ℓ channel

Process	ggF SR	Mixed SR	EW SR
$gg \to (H^* \to) ZZ$	341 ± 117	42.5 ± 14.9	11.8 ± 4.3
$gg \to H^* \to ZZ$	32.6 ± 9.07	3.68 ± 1.03	1.58 ± 0.47
$gg \to ZZ$	345 ± 119	43.0 ± 15.2	11.9 ± 4.4
$qq \to (H^* \to) ZZ + 2j$	23.2 ± 1.0	2.03 ± 0.16	9.89 ± 0.96
$qq \to ZZ$	1878 ± 151	135 ± 23	22.0 ± 8.3
Other backgrounds	50.6 ± 2.5	1.79 ± 0.16	1.65 ± 0.16
Total expected (SM)	2293 ± 209	181 ± 29	45.3 ± 10.0
Observed	2327	178	50

Off-Shell Higgs Production

- Observed and expected yields in the $2\ell 2$ channel

Process	ggF SR	Mixed SR	EW SR
$gg \to (H^* \to) ZZ$	210 ± 53	19.7 ± 4.9	4.29 ± 1.10
$gg \to H^* \to ZZ$	111 ± 26	10.9 ± 2.5	3.26 ± 0.82
$gg \to ZZ$	251 ± 66	23.4 ± 6.2	5.31 ± 1.46
$qq \to (H^* \to) ZZ + 2j$	14.0 ± 3.0	1.63 ± 0.17	4.46 ± 0.50
$qq \to ZZ$	1422 ± 112	80.4 ± 11.9	7.74 ± 2.99
WZ	678 ± 54	51.9 ± 6.9	7.89 ± 2.50
Z+jets	62.3 ± 24.3	7.51 ± 6.94	0.62 ± 0.54
Non-resonant-$\ell\ell$	106 ± 39	9.17 ± 2.73	1.55 ± 0.42
Other backgrounds	22.6 ± 5.2	1.62 ± 0.25	1.40 ± 0.10
Total expected (SM)	2515 ± 165	172 ± 17	28.0 ± 4.1
Observed	2496	181	27

$$m_{\mathrm{T}}^{ZZ} \equiv \sqrt{\left[\sqrt{m_Z^2 + \left(p_{\mathrm{T}}^{\ell\ell}\right)^2} + \sqrt{m_Z^2 + \left(E_{\mathrm{T}}^{\mathrm{miss}}\right)^2}\right]^2 - \left|\vec{p}_{\mathrm{T}}^{\,\ell\ell} + \vec{E}_{\mathrm{T}}^{\mathrm{miss}}\right|^2}$$

Off-Shell Higgs Production

- Fit results and dominant systematics

Normalization factor	Fitted value
μ_{qqZZ}	1.11 ± 0.07
μ^{1j}_{qqZZ}	0.90 ± 0.10
μ^{2j}_{qqZZ}	0.88 ± 0.26
$\mu_{3\ell}$	1.06 ± 0.03
$\mu^{1j}_{3\ell}$	0.92 ± 0.10
$\mu^{2j}_{3\ell}$	0.75 ± 0.19
μ_{Zj}	0.90 ± 0.19
$\mu_{e\mu}$	1.08 ± 0.09

Systematic Uncertainty Fixed	$\mu_{\text{off-shell}}$ value at which $-2\ln\lambda(\mu_{\text{off-shell}}) = 4$
Parton shower uncertainty for $gg \to ZZ$ (normalisation)	2.26
Parton shower uncertainty for $gg \to ZZ$ (shape)	2.29
NLO EW uncertainty for $qq \to ZZ$	2.27
NLO QCD uncertainty for $gg \to ZZ$	2.29
Parton shower uncertainty for $qq \to ZZ$ (shape)	2.29
Jet energy scale and resolution uncertainty	2.26
None	2.30

Off-Shell Higgs Production and Width

Due to the quadratic parameterisation of the yield as a function of the parameter of interest, the distribution of the test statistic $-2\ln\lambda$ is slightly different from the asymptotic χ^2 distribution predicted by Wilks' theorem [87]. Therefore confidence intervals on $\mu_{\text{off-shell}}$ are built based on the Neyman construction [88] using the distribution of $-2\ln\lambda$ for different values of the parameter of interest. The distributions of $-2\ln\lambda$ are estimated using simulated events sampled from the likelihood model of the analysis, profiled to the best fit results from data. The resulting confidence intervals are 5–10% more conservative than those obtained by assuming that the asymptotic assumption is correct. The curves in Figure 6(a) represent these true 68 and 95% confidence intervals.

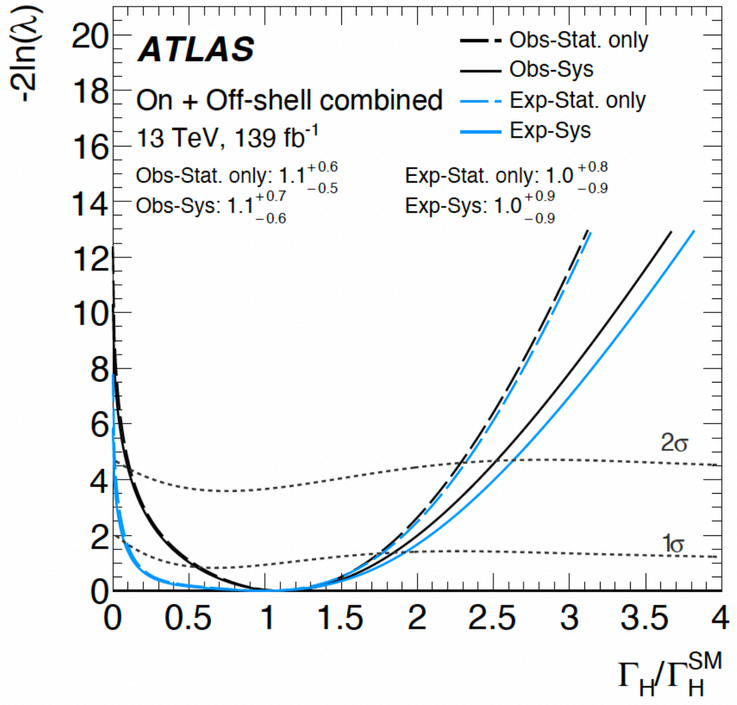

Measuring CP properties of Higgs boson interactions with τ leptons

Table 1: Notation for the dominant leptonic and hadronic τ-lepton decay modes used and their branching fractions. The symbol '$\ell^{\pm}$' stands for $e^{\pm}$ or $\mu^{\pm}$, and '$h^{\pm}$' includes $\pi^{\pm}$ and $K^{\pm}$. The parentheses show the hadronic decays involving $\pi^{\pm}$ and their corresponding branching fractions.

Notation	Decay mode	Branching fraction
ℓ	$\ell^{\pm}\bar{\nu}\nu$	35.2%
1p0n	$h^{\pm}\nu$ ($\pi^{\pm}\nu$)	11.5% (10.8%)
1p1n	$h^{\pm}\pi^0\nu$ ($\pi^{\pm}\pi^0\nu$)	25.9% (25.5%)
1pXn	$h^{\pm} \geq 2\pi^0\nu$ ($\pi^{\pm}2\pi^0\nu$)	10.8% (9.3%)
3p0n	$3h^{\pm}\nu$ ($3\pi^{\pm}\nu$)	9.8% (9.0%)

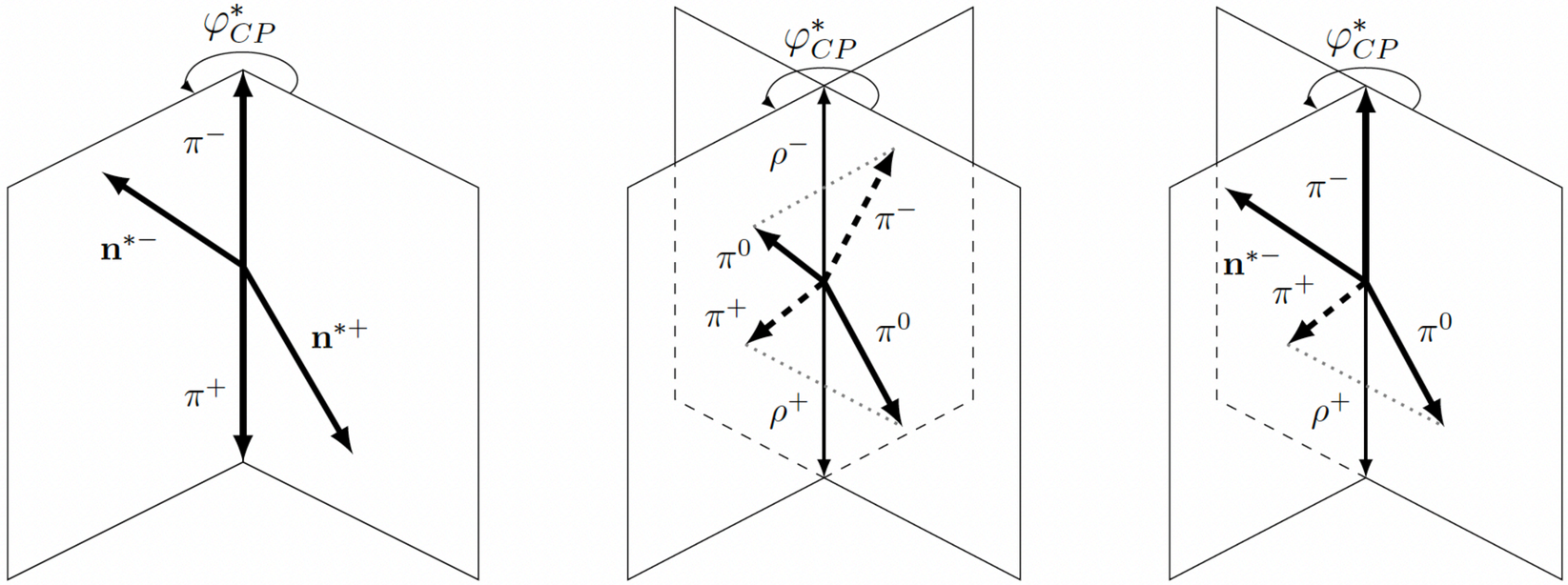

(a) $H \to \tau^+\tau^- \to \pi^+\pi^- + 2\nu$ (b) $H \to \tau^+\tau^- \to \pi^+\pi^0\nu\pi^-\pi^0\nu$ (c) $H \to \tau^+\tau^- \to \pi^+\pi^0\nu\pi^-\nu$

Measuring CP properties of Higgs boson interactions with τ leptons

Set of nuisance parameters	Impact on ϕ_τ [degrees]
Jet energy scale	3.4
Jet energy resolution	2.5
Pile-up jet tagging	0.5
Jet flavour tagging	0.2
$E_{\mathrm{T}}^{\mathrm{miss}}$	0.4
Electron	0.3
Muon	0.9
τ_{had} reconstruction	1.0
Misidentified τ	0.6
τ_{had} decay mode classification	0.3
π^0 angular resolution and energy scale	0.2
Track ($\pi^\pm$, impact parameter)	0.7
Luminosity	0.1
Theory uncertainty in $H \to \tau\tau$ processes	1.5
Theory uncertainty in $Z \to \tau\tau$ processes	1.1
Simulated background sample statistics	1.4
Signal normalisation	1.4
Background normalisation	0.6
Total systematic uncertainty	5.2
Data sample statistics	15.6
Total	16.4

Fitted parameters	Observed	Expected
ϕ_τ	$9° \pm 16°$	$0° \pm 28°$
$\mu_{\tau\tau}$	$1.02^{+0.20}_{-0.20}$	$1.00^{+0.21}_{-0.21}$
$\mathrm{NF}^{\mathrm{Boost\_1}}_{Z\to\tau\tau}$	1.01 ± 0.05	1.00 ± 0.04
$\mathrm{NF}^{\mathrm{Boost\_0}}_{Z\to\tau\tau}$	1.02 ± 0.05	1.00 ± 0.05
$\mathrm{NF}^{\mathrm{VBF\_1}}_{Z\to\tau\tau}$	1.04 ± 0.08	1.00 ± 0.08
$\mathrm{NF}^{\mathrm{VBF\_0}}_{Z\to\tau\tau}$	0.95 ± 0.07	1.00 ± 0.08

Wilson Coefficients

- Taken from Valentina Cairo's talk

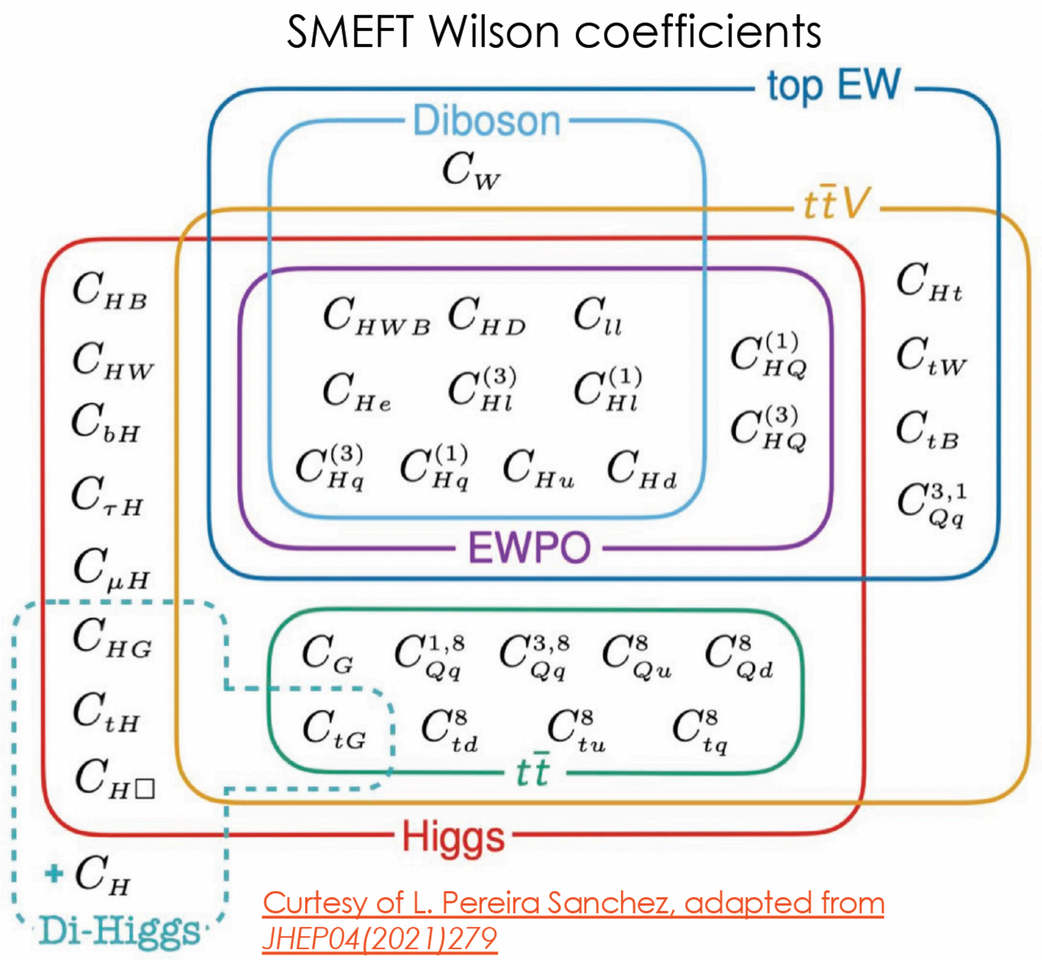

Curtesy of L. Pereira Sanchez, adapted from *JHEP04(2021)279*

$$\mathcal{L}_{\text{SMEFT}} = \mathcal{L}_{\text{SM}} + \sum_i \frac{c_i}{\Lambda^2} O_i^{(6)}$$

Probing the CP-odd Component with H→ZZ*→4ℓ

Table 1: SMEFT CP-odd dimension-six operators in the Warsaw and Higgs bases relevant for the measurement of CP-invariance in the $H \to ZZ^* \to 4\ell$ decay channel. The gauge field strength tensors are denoted $W^I_{\mu\nu}$ and $B_{\mu\nu}$, while Φ is the scalar doublet Higgs boson field. The photon and Z-boson field strength tensors after electroweak symmetry breaking are denoted as $A_{\mu\nu}$ and $Z_{\mu\nu}$, respectively, and h denotes the massive Higgs field after electroweak symmetry breaking. Combinations of couplings in one basis can be translated into equivalent combinations of couplings from the other basis that describe the same phenomena [36, 37].

Operator	Structure	Coupling
	Warsaw Basis	
$O_{\Phi\tilde{W}}$	$\Phi^\dagger\Phi\tilde{W}^I_{\mu\nu}W^{\mu\nu I}$	$c_{H\widetilde{W}}$
$O_{\Phi\tilde{W}B}$	$\Phi^\dagger\tau^I\Phi\tilde{W}^I_{\mu\nu}B^{\mu\nu}$	$c_{H\widetilde{W}B}$
$O_{\Phi\tilde{B}}$	$\Phi^\dagger\Phi\tilde{B}_{\mu\nu}B^{\mu\nu}$	$c_{H\widetilde{B}}$
	Higgs Basis	
$O_{hZ\tilde{Z}}$	$hZ_{\mu\nu}\tilde{Z}^{\mu\nu}$	$\widetilde{c}_{zz}$
$O_{hZ\tilde{A}}$	$hZ_{\mu\nu}\tilde{A}^{\mu\nu}$	$\widetilde{c}_{z\gamma}$
$O_{hA\tilde{A}}$	$hA_{\mu\nu}\tilde{A}^{\mu\nu}$	$\widetilde{c}_{\gamma\gamma}$

Finally, a common parameterization used in existing experimental searches for CP-violation at the HVV vertex [10, 30] assumes a single BSM CP-odd Higgs boson coupling denoted by $\widetilde{d}$. In [10], it was considered that the different contributions from the various electroweak gauge-boson fusion processes could not be distinguished experimentally, and assumed that the BSM CP-odd Higgs boson couplings $c_{H\widetilde{W}}$ and $c_{H\widetilde{B}}$ in the Warsaw basis are equal, leading to the remaining coupling $c_{H\widetilde{W}B}$ being zero. The CP-odd parameter $\widetilde{d}$ is related to the Warsaw-basis couplings by the parameterization $c_{H\widetilde{W}} = c_{H\widetilde{B}} = \frac{\Lambda^2}{v^2}\widetilde{d}$, where v is the Higgs boson vacuum expectation value. In the Higgs basis, it is equivalent to the direction $\widetilde{c}_{z\gamma} = 0$, $\widetilde{c}_{\gamma\gamma} = \sin^2\theta_W \cos^2\theta_W \widetilde{c}_{zz}$, where θ_W is the Weinberg angle.

Probing the CP-odd Component with H→ZZ*→4ℓ

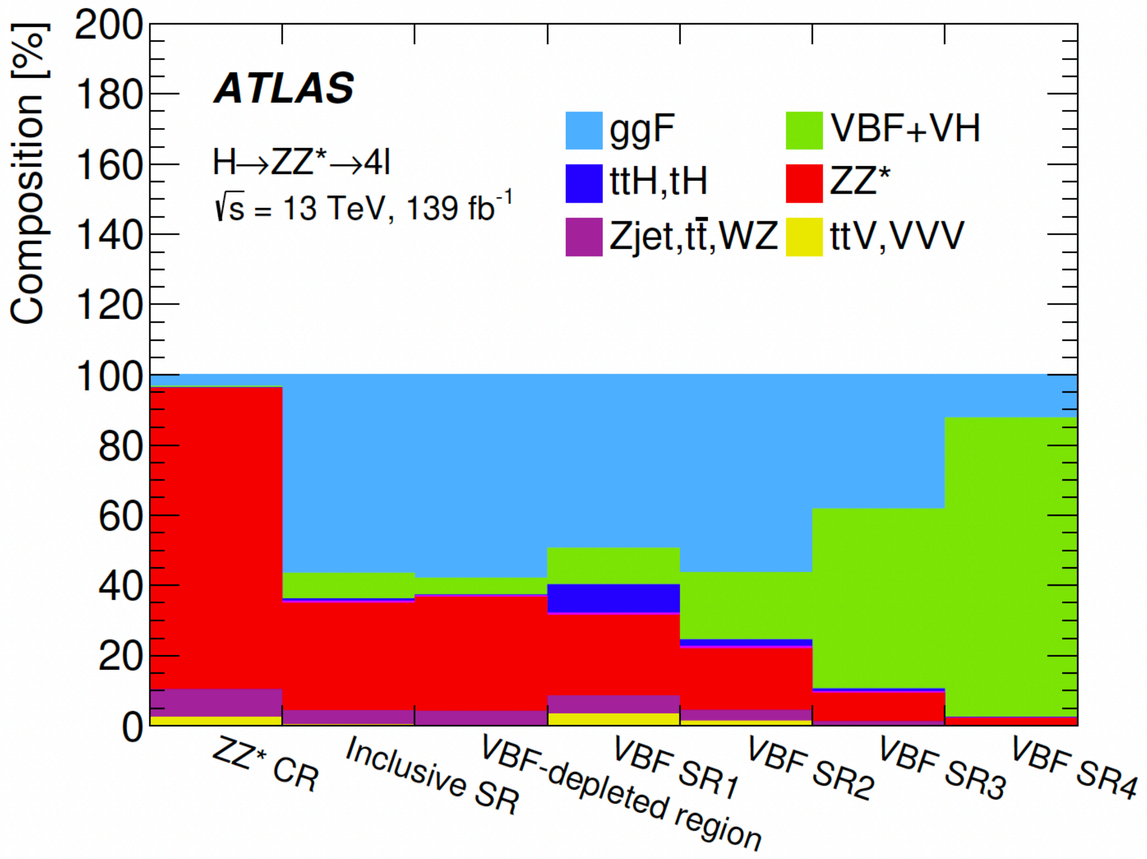

Figure 2: The composition of the predicted event yield in the event categories used for the direct EFT coupling measurements. The contribution from bbH is negligible and not visible in the plot. The MC statistical uncertainty in the fraction of each component is not shown but is below the 1% level.

Probing the CP-odd Component with H→ZZ*→4ℓ

Table 3: The numbers of expected and observed events in the event categories for the direct CP measurement, in the mass range 115 GeV $< m_{4\ell} <$ 130 GeV. The sum of the number of expected SM Higgs boson events and the estimated background yields is compared with the data. Combined statistical and systematic uncertainties are included for the predictions. The Inclusive SR, used in the decay-only fit, is composed of the VBF-depleted Region and VBF SR1 to SR4.

	ZZ^* CR	Inclusive SR	VBF-depleted Region	VBF SR1	VBF SR2	VBF SR3	VBF SR4
ggF	8.2 ± 1.3	181 ± 12	165 ± 12	$7.5^{+3.0}_{-2.4}$	$5.6^{+1.8}_{-1.5}$	2.2 ± 0.6	0.49 ± 0.17
bbH	$0.087^{+0.016}_{-0.015}$	1.85 ± 0.05	1.65 ± 0.05	0.11 ± 0.01	$0.072^{+0.010}_{-0.009}$	$0.020^{+0.005}_{-0.003}$	< 0.01
VBF/VH	1.39 ± 0.16	23.8 ± 0.7	13.8 ± 0.6	$1.60^{+0.09}_{-0.08}$	1.89 ± 0.11	3.01 ± 0.18	3.5 ± 0.4
ttH,tH	$0.22^{+0.03}_{-0.04}$	$1.89^{+0.21}_{-0.22}$	0.44 ± 0.05	1.22 ± 0.14	0.179 ± 0.023	$0.046^{+0.009}_{-0.010}$	< 0.01
ttV,VVV	6.79 ± 0.13	1.31 ± 0.06	0.62 ± 0.04	0.53 ± 0.04	0.150 ± 0.020	< 0.01	< 0.01
ZZ^*	229^{+20}_{-25}	98^{+6}_{-9}	92^{+6}_{-8}	$3.5^{+1.3}_{-1.7}$	1.7 ± 0.6	$0.48^{+0.16}_{-0.15}$	$0.086^{+0.025}_{-0.028}$
Zjet,$t\bar{t}$,WZ	21 ± 5	13 ± 4	12 ± 3	0.8 ± 0.9	0.3 ± 0.6	0.07 ± 0.26	0.01 ± 0.09
Total SM	267^{+21}_{-26}	321^{+14}_{-15}	286^{+14}_{-15}	15 ± 3	$9.9^{+2.0}_{-1.7}$	5.9 ± 0.7	4.1 ± 0.5
Data	294	311	276	14	9	4	8

Probing the CP-odd Component with H→ZZ*→4ℓ

Table 4: The expected 95% confidence intervals of production-only, decay-only and combined production and decay likelihood scans for the CP-odd Wilson coefficients in the Warsaw and Higgs bases for an integrated luminosity of 139 fb^{-1} at $\sqrt{s}$ = 13 TeV. Only one Wilson coefficient is fitted at a time while all others are set to zero. Limits denoted by '–' indicates no sensitivity. All couplings scale as $1/\Lambda^2$ with the assumed value of Λ = 1 TeV.

EFT coupling	Expected 95% CL		
	production-only	decay-only	combined
$c_{H\widetilde{B}}$	–	±0.37	–
$c_{H\widetilde{W}B}$	–	±0.72	–
$c_{H\widetilde{W}}$	±4.8	±1.34	±1.27
$\widetilde{d}$	±0.63	±0.018	±0.019
$\widetilde{c}_{zz}$	±2.4	–	–
$\widetilde{c}_{z\gamma}$	±6.6	±0.76	±0.80
$\widetilde{c}_{\gamma\gamma}$	–	±0.76	–

Probing the CP-odd Component with H→ZZ*→4ℓ

Table 5: The expected and observed confidence intervals at 68% and 95% CL for the CP-odd Wilson coefficients for an integrated luminosity of 139 fb^{-1} at $\sqrt{s}$ = 13 TeV. Only one Wilson coefficient is fitted at a time while all others are set to zero. The observed best fit value and p-value for agreement with the SM is provided. The last column indicates whether the limits come from production (prod), decay or a combination of production and decay (comb). All couplings scale as $1/\Lambda^2$ with the assumed value of Λ = 1 TeV.

EFT coupling	Expected		Observed		Best-fit	SM	Fit type
parameter	68% CL	95% CL	68% CL	95% CL	value	p-value	
$c_{H\widetilde{B}}$	[−0.18, 0.19]	[−0.37, 0.37]	[−0.42, 0.31]	[−0.61, 0.54]	−0.078	0.86	decay
$c_{H\widetilde{W}B}$	[−0.36, 0.36]	[−0.72, 0.72]	[−0.56, 0.53]	[−0.97, 0.98]	−0.017	0.99	decay
$c_{H\widetilde{W}}$	[−0.63, 0.63]	[−1.26, 1.28]	[−0.07, 1.09]	[−0.81, 1.54]	0.60	0.37	comb
$\widetilde{d}$	[−0.009, 0.009]	[−0.018, 0.018]	[−0.017, 0.014]	[−0.026, 0.025]	−0.003	0.86	decay
$\widetilde{c}_{zz}$	[−0.77, 0.79]	[−2.4, 2.4]	[0.37, 1.21]	[−1.20, 1.75]	0.78	0.11	prod
$\widetilde{c}_{z\gamma}$	[−0.47, 0.47]	[−0.76, 0.76]	[−0.54, 0.54]	[−0.84, 0.83]	0.083	0.93	decay
$\widetilde{c}_{\gamma\gamma}$	[−0.38, 0.38]	[−0.76, 0.77]	[−0.52, 0.48]	[−0.99, 0.93]	−0.01	0.99	decay

Probing the CP Nature of the Higgs-top Yukawa Coupling

Table 1: Definition of the CRs and TRs according to the number of jets and b-tagged jets using different b-tagging selection criteria, and the number of boosted Higgs boson candidates. For CRs, the bottom row indicates the observables used in the fit to data in the corresponding regions. For the $\mathrm{TR}_{\mathrm{boosted}}$ region, the b-tagged jets flagged with † are not constituents of the boosted Higgs boson candidate. Events must pass $N_{b\text{-tag}}$ requirements for each b-tagging selection criteria.

Region		Dilepton				ℓ+jets			
		$\mathrm{TR}^{\geq 4j,\geq 4b}$	$\mathrm{CR}^{\geq 4j,3b}_{\mathrm{hi}}$	$\mathrm{CR}^{\geq 4j,3b}_{\mathrm{lo}}$	$\mathrm{CR}^{3j,3b}_{\mathrm{hi}}$	$\mathrm{TR}^{\geq 6j,\geq 4b}$	$\mathrm{CR}^{5j,\geq 4b}_{\mathrm{hi}}$	$\mathrm{CR}^{5j,\geq 4b}_{\mathrm{lo}}$	$\mathrm{TR}_{\mathrm{boosted}}$
N_{jets}		≥ 4			$=3$	≥ 6	$=5$		≥ 4
$N_{b\text{-tag}}$	@85%	–				≥ 4			
	@77%	–				–			$\geq 2^{\dagger}$
	@70%	≥ 4	$=3$			≥ 4			–
	@60%	–	$=3$	<3	$=3$	–	≥ 4	<4	–
$N_{\mathrm{boosted\ cand.}}$		–				0			≥ 1
Fit observable		–	Yield			–	$\Delta R^{\mathrm{avg}}_{bb}$		–

Probing the CP Nature of the Higgs-top Yukawa Coupling

$$b_2 = \frac{(\vec{p}_1 \times \hat{z}) \cdot (\vec{p}_2 \times \hat{z})}{|\vec{p}_1||\vec{p}_2|}, \quad \text{and} \quad b_4 = \frac{(\vec{p}_1 \cdot \hat{z})(\vec{p}_2 \cdot \hat{z})}{|\vec{p}_1||\vec{p}_2|},$$

where $\vec{p}_i$ with $i = 1, 2$ are the momentum three-vectors of the two top quarks in the events and $\hat{z}$ is a unit vector in the direction of the beamline and defines the z-axis [15]. The b_4 observable exploits the enhanced production of top quarks travelling in opposite longitudinal directions and closer to the beamline in CP-odd $t\bar{t}H$ production. The observable b_2 relies simultaneously on the smaller azimuthal separation of top quarks and on their larger longitudinal fraction of momentum in CP-odd $t\bar{t}H$ production. The calculation of b_2 is performed in the $t\bar{t}H$ rest frame [28], which enhances the discrimination power.

Probing the CP Nature of the Higgs-top Yukawa Coupling

Table 2: Summary of the selections used to define SRs and CRs from the TRs, based on the classification BDT score. In the boosted region, the selection requirement is applied and rejected events are removed entirely from further analysis. In the dilepton channel, events with failed reconstruction due to absence of a real solution from the neutrino weighting are categorised into an additional region known as $\mathrm{CR}^{\geq 4j,\geq 4b}_{\text{no-reco}}$. The fitted discriminating variable in each region is indicated in the last column.

Channel (TR)	Final SRs and CRs	Classification BDT selection	Fitted observable
Dilepton ($\mathrm{TR}^{\geq 4j,\geq 4b}$)	$\mathrm{CR}^{\geq 4j,\geq 4b}_{\text{no-reco}}$	–	$\Delta\eta_{\ell\ell}$
	$\mathrm{CR}^{\geq 4j,\geq 4b}$	$\mathrm{BDT}^{\geq 4j,\geq 4b} \in [-1, -0.086)$	b_4
	$\mathrm{SR}^{\geq 4j,\geq 4b}_1$	$\mathrm{BDT}^{\geq 4j,\geq 4b} \in [-0.086, 0.186)$	b_4
	$\mathrm{SR}^{\geq 4j,\geq 4b}_2$	$\mathrm{BDT}^{\geq 4j,\geq 4b} \in [0.186, 1]$	b_4
ℓ+jets ($\mathrm{TR}^{\geq 6j,\geq 4b}$)	$\mathrm{CR}^{\geq 6j,\geq 4b}_1$	$\mathrm{BDT}^{\geq 6j,\geq 4b} \in [-1, -0.128)$	b_2
	$\mathrm{CR}^{\geq 6j,\geq 4b}_2$	$\mathrm{BDT}^{\geq 6j,\geq 4b} \in [-0.128, 0.249)$	b_2
	$\mathrm{SR}^{\geq 6j,\geq 4b}$	$\mathrm{BDT}^{\geq 6j,\geq 4b} \in [0.249, 1]$	b_2
ℓ+jets ($\mathrm{TR}_{\text{boosted}}$)	$\mathrm{SR}_{\text{boosted}}$	$\mathrm{BDT}^{\text{boosted}} \in [-0.05, 1]$	$\mathrm{BDT}^{\text{boosted}}$

Probing the CP Nature of the Higgs-top Yukawa Coupling